

Aus der medizinischen Klinik und Poliklinik IV  
der Ludwig-Maximilians-Universität München

Klinischer Direktor: Prof. Dr. med. Martin Reincke

**Preclinical progress and first translational research steps for a  
novel liposomal chemotherapy against  
adrenocortical carcinoma**

Dissertation

zum Erwerb des Doktorgrades der Humanbiologie an der Medizinischen  
Fakultät der Ludwig-Maximilians-Universität zu München

vorgelegt von

Sara Jung

aus

München

2018



Mit Genehmigung der Medizinischen Fakultät der  
Universität München

Berichterstatter:	Prof. Dr. med. Felix Beuschlein
Mitberichterstatter:	Prof. Dr. med. Stefan R. Bornstein Prof. Dr. med. Dietrich von Schweinitz Prof. Dr. med. Christine Spitzweg
Mitbetreuung durch den promovierten Mitarbeiter:	Dr. hum. biol. Constanze Hantel
Dekan:	Prof. Dr. med. dent. Reinhard Hickel
Tag der mündlichen Prüfung:	25.05.2018



## Eidesstattliche Versicherung

# Jung, Sara

---

Name, Vorname

Ich erkläre hiermit an Eides statt,

dass ich die vorliegende Dissertation mit dem Thema

**Preclinical progress and first translational research steps for a novel liposomal chemotherapy against adrenocortical carcinoma**

selbständig verfasst, mich außer der angegebenen keiner weiteren Hilfsmittel bedient und alle Erkenntnisse, die aus dem Schrifttum ganz oder annähernd übernommen sind, als solche kenntlich gemacht und nach ihrer Herkunft unter Bezeichnung der Fundstelle einzeln nachgewiesen habe.

Ich erkläre des Weiteren, dass die hier vorgelegte Dissertation nicht in gleicher oder in ähnlicher Form bei einer anderen Stelle zur Erlangung eines akademischen Grades eingereicht wurde.

München, 19.06.2018

---

Ort, Datum

Sara Jung

---

Unterschrift Doktorandin/Doktorand



Für meine Familie



## Table of contents

<b>1. Introduction.....</b>	<b>11</b>
1.1 Current clinical situation and medical treatment options for ACC.....	11
1.2 Liposomal chemotherapies.....	14
1.3 Liposomal chemotherapeutic protocols as novel therapeutic approaches for ACC.....	17
1.4 Human xenograft models of ACC.....	19
1.5 Circulating micro-RNAs as marker for therapeutic efficacy in ACC.....	21
1.6 General aim.....	23
<b>2. Materials and Methods.....</b>	<b>24</b>
2.1 Reagents and equipment.....	24
2.2 Cell culture and tumor cell preparation for tumor induction.....	33
2.3 Animal experiments.....	34
2.3.1 Housing conditions.....	34
2.3.2 Preclinical tumor models and tumor induction.....	34
2.3.2.1 Cell-line based SW-13 tumor model.....	35
2.3.2.2 Xenograft based SJ-ACC3 tumor model.....	35
2.3.3 Therapeutic experiments.....	36
2.3.3.1 Preparation of therapeutic drugs.....	36
2.3.3.2 Therapeutic treatments and sample collection.....	37
2.3.4 Histology and immunohistochemistry.....	40

2.3.4.1	Paraffin embedding of tissues.....	40
2.3.4.2	Preparation of tissue for immunohistochemistry and histology.....	40
2.3.4.3	Immunohistological and histological evaluation.....	41
2.3.4.4	Ki67 immunohistochemistry.....	41
2.3.4.5	TUNEL immunohistochemistry.....	42
2.3.4.6	Hematoxylin/Eosin staining.....	42
2.4	Molecular Analyses.....	43
2.5	Clinical experiments.....	45
2.6	Statistical analysis.....	45
<b>3.</b>	<b>Results.....</b>	<b>46</b>
3.1	Short-term therapeutic efficacy.....	46
3.1.1	Evaluation of the total number of tumor cells.....	46
3.1.2	Investigation of apoptosis.....	48
3.1.3	Histological evaluation of necrosis in tumor tissues.....	48
3.2	Long-term therapeutic efficacy.....	51
3.3	Tolerability and off-target profiles.....	53
3.4	Analysis of leukocytes upon short-term treatment.....	53
3.5	Analysis of survival and lethal side-effects upon long-term treatment.....	54
3.6	Analysis of hearts and kidneys.....	55
3.7	Circulating miR-210 as potential biomarker for therapeutic efficacy.....	57

3.8	Clinical data.....	59
<b>4.</b>	<b>Discussion.....</b>	<b>61</b>
4.1	Therapeutic efficacy of liposomal EDP-M regimens.....	62
4.2	Off-target profiles of liposomal EDP-M regimens in preclinical tumor xenografts .....	64
4.3	MiR-483-5p and miR-210 as therapeutic biomarkers for ACC .....	66
4.4	Liposomally modified EDP-M in clinics .....	68
4.5	Perspectives and outlook .....	69
<b>5.</b>	<b>Summary.....</b>	<b>70</b>
	<b>Zusammenfassung.....</b>	<b>71</b>
<b>6.</b>	<b>References .....</b>	<b>72</b>
<b>7.</b>	<b>Appendix.....</b>	<b>79</b>
7.1	Abbreviations .....	79
7.2	Acknowledgements .....	82

## **1. Introduction**

### **1.1 Current clinical situation and medical treatment options for ACC**

Adrenocortical carcinoma (ACC) is a very rare but highly heterogeneous malignancy with an annual incidence of 0.7 to 2.0 cases per million [1]. This tumor entity is characterized by a very aggressive clinical behavior [2] and reveals a bimodal age distribution pattern with peaks in early childhood as well as in the fourth and fifth decade of life [3, 4].

In patients without clinical symptoms of hormone hypersecretion, local tumor progression and spreading into the surrounding viscera often lead to unspecific symptoms as back pain, abdominal discomfort as well as nausea and vomiting [4]. However, in approximately 60% of cases patients display symptoms with evidence of adrenal steroid hormone excess most frequently presented as rapid progressing Cushing's syndrome with or without virilization due to excessive androgen production [3, 4]. Such patterns of abnormal hormonal secretion can be highly variable depending on tumor size, stage and differentiation which leads to delayed diagnosis as syndromes of hormonal excess are often not easily recognized [4]. Thus, advanced ACC defined as tumor stage III (in the case of local tumor spread) or as stage IV (in the presence of distant metastases), represent 18-26% and 21-46% of adrenocortical tumors at diagnosis, respectively [2]. The individual tumor stage at initial diagnosis, very recently updated by the modified ENSAT (mENSAT) classification, is one of the keystones for prognostic stratification [2]. As such, also the number of organs affected by the tumor and the involved lymph nodes have important prognostic value [2].

The prognosis for ACC revealing an advanced tumor stage III and IV at diagnosis is dismal with a 5-year overall survival of 50% and 2%, respectively [2]. Furthermore, there is a strong tendency towards rapid progression in advanced ACC while disease stabilization for longer than three months is rarely observed [1]. Currently, a complete tumor resection represents the only curative approach for localized adrenocortical tumors and therapeutic intervention must be considered to be palliative in case of unresectable or metastatic tumors [5]. Although the majority of ACC is surgically resectable at presentation, up to 85% of tumors relapse after radical resection [6] as the high growth potential of this endocrine neoplasm in many cases leads to already advanced metastasized tumors at initial ACC diagnosis [4, 7].

Medical therapy of locally advanced or metastasized ACC is limited to common cytostatic drugs which are usually combined with mitotane (*o,p'*DDD, 1,1-dichloro-2(*o*-chlorophenyl)-2-(*p*-chlorophenyl)ethane), a substance exhibiting adrenolytic effects [4, 5, 8]. Of pivotal importance for the management of this rare disease was the first international randomized trial in locally advanced adrenocortical carcinoma treatment (FIRM-ACT [9], Fig. 1).

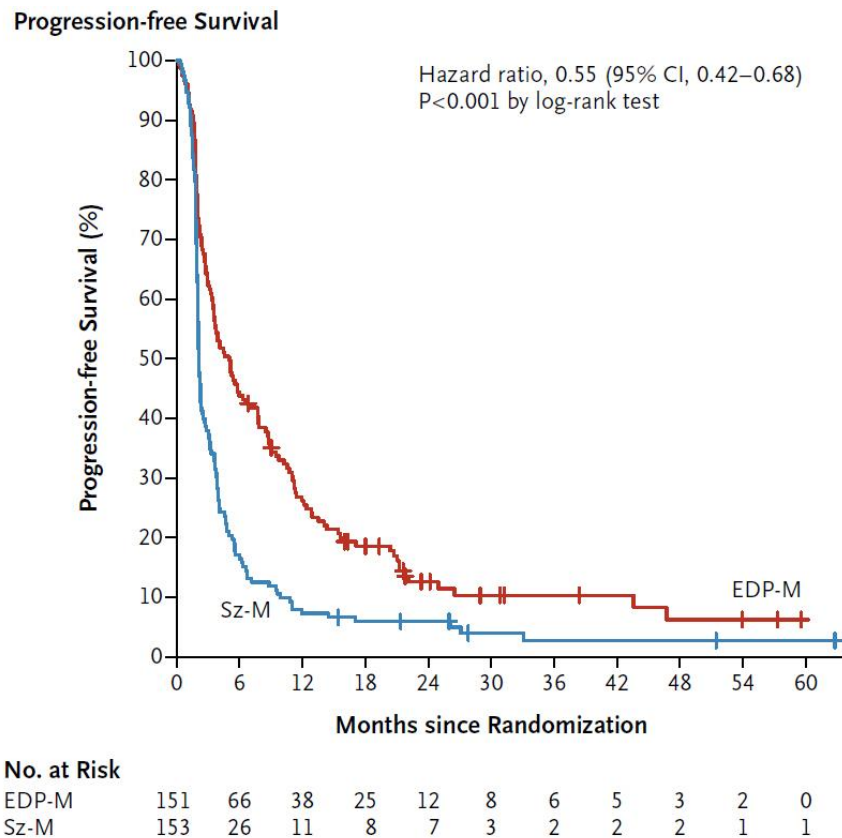


**Fig. 1:** Progression-free survival during first-line therapy with streptozotocin (Sz) and mitotane (M) versus etoposide, doxorubicin and cisplatin (EDP) plus mitotane (M) (adapted from [9]).

For the first time, the two most promising therapy regimens for advanced ACC were compared in a large cohort of patients: Streptozotocin and mitotane (Sz-M) versus etoposide, doxorubicin and cisplatin plus mitotane (EDP-M) [9]. Compared to Sz-M, the EDP-M combination chemotherapy protocol led to higher response rates and longer progression-free survival (Fig. 1) [9]. In accordance with this clinical trial, EDP-M was defined as the current treatment standard for advanced and metastasized ACC [9]. Nevertheless, this prospective trial also clearly evidenced that the therapeutic efficacy of EDP-M treatment is still poor and very unsatisfactory (Fig. 1).

Moreover, the combined administration of potent cytostatic drugs together with mitotane results in a highly toxic regimen with severe dose-limiting side-effects. As shown in figure 2, treatment with EDP-M leads to severe off-target actions. Such adverse effects are characterized by hematological toxicities with dose-limiting leucopenia, gastrointestinal and other toxicities which also include irreversible cardiotoxic and nephrotoxic events [9, 10].

Event	EDP-M (N = 148)	Sz-M (N = 149)
	<i>no. of patients (%)</i>	
Any serious adverse event	86 (58.1)	62 (41.6)
Adrenal insufficiency	5 (3.4)	1 (0.7)
Bone marrow toxicity	17 (11.5)	3 (2.0)
Cardiovascular or thromboembolic event	10 (6.8)	0
Fatigue or general health deterioration	8 (5.4)	7 (4.7)
Gastrointestinal disorder	6 (4.1)	12 (8.1)
Impaired liver function	0	7 (4.7)
Impaired renal function	1 (0.7)	6 (4.0)
Infection	10 (6.8)	4 (2.7)
Neurologic toxicity	5 (3.4)	4 (2.7)
Respiratory disorder	9 (6.1)	5 (3.4)
Other	15 (10.1)	13 (8.7)

**Fig. 2:** Adverse effects of streptozotocin (Sz) and mitotane (M) versus etoposide, doxorubicin and cisplatin (EDP) plus mitotane (M) which were both investigated in the FIRM-ACT study (adapted from [9]).

In particular, the cytostatic drug doxorubicin is well known to induce congestive heart failure as well as cardiomyopathy even many years after treatment [11, 12]. Thus, the cumulative dose of doxorubicin has to be limited in clinical practice. This fact creates a dilemma of balancing suboptimal oncologic therapy with a proven beneficial treatment against the risk of inducing irreversible cardiotoxic effects [11]. Also, the significant risk of cisplatin-induced nephrotoxicity impedes the use of higher doses of cisplatin to maximize its anti-tumoral effects in therapeutic treatment regimens [13]. The decisive and most important objective of novel therapeutic approaches for advanced ACC thus consists of developing treatment regimens with reduced off-target profiles while maintaining or even increasing therapeutic efficacy.

## 1.2 Liposomal chemotherapies

In recent years, liposomal chemotherapies have been established to improve off-target profiles as well as therapeutic efficacy. Compared to their conventional free formulation, liposomal drugs have slower releasing rates and sustained bioavailability [14, 15]. Moreover, liposomes can be grafted using the biocompatible polymer polyethylene glycol (PEG) which is inert and forms a protective layer on the surface (see Fig. 3) [16, 17]. Such modification using PEG prevents recognition of liposomes by opsonins and leads to a reduced clearance by the reticuloendothelial system (RES) [16].

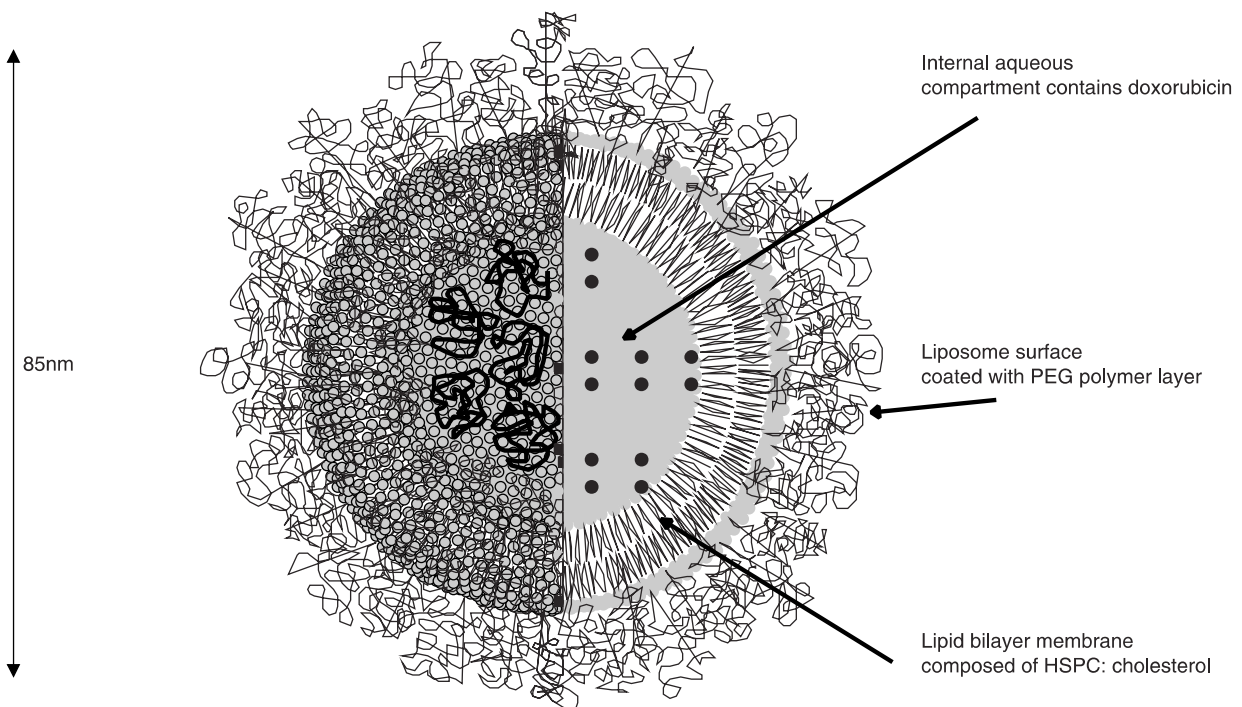


**Fig. 3:** Cross-sectional view of a PEGylated (polyethylene glycol) liposomal formulation of doxorubicin (doxil®, caelyx™). Polymer groups of polyethylene glycol form a protective layer on the liposome surface and provide additional stability, HSPC = hydrogenated soy phosphatidylcholine (adapted from [17]).

These so-called “sterically stabilized liposomes” reveal an increased half-life in the plasma compartment [18]. Using modifications as PEGylated phospholipids, an extension of the terminal half-life of such long-circulating liposomes from a time-scale of minutes to days has been demonstrated [16, 19]. Small-molecule properties of most conventional chemotherapeutic

agents lead to a high volume of distribution and thereby to significant toxicity for normal tissues as well as low drug levels at the tumor site. Such biodistribution patterns are modified by liposomal encapsulation which leads to decreased volumes of distribution of cytotoxic drugs and improved delivery to the site of action [17, 19].

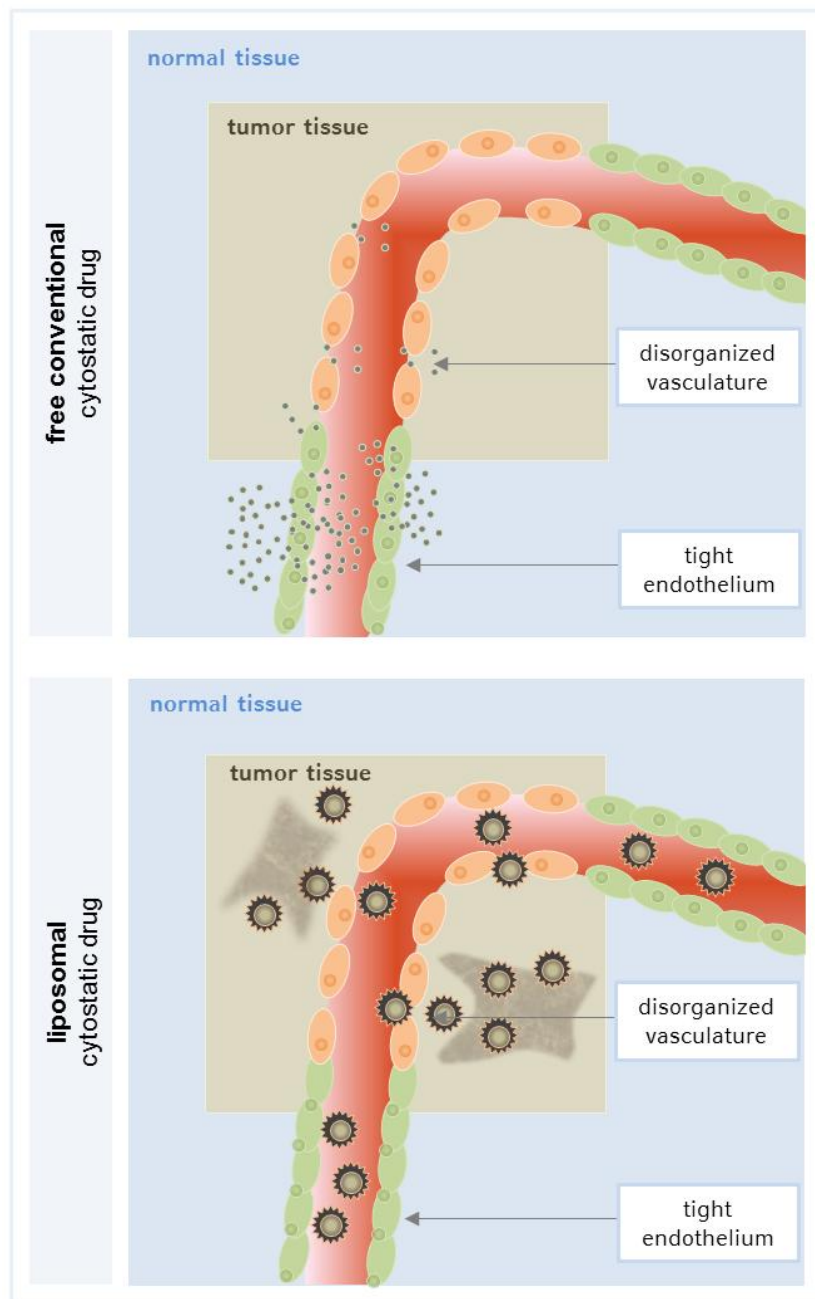


**Fig. 4:** Passive tumor targeting of long-circulating liposomal cytostatic drugs occurs by the enhanced permeability and retention (EPR) effect. The angiogenic vasculature in the tumor site is hyperpermeable and enables a preferential extravasation of macromolecular liposomal cytostatic drugs (adapted from [20]).

In particular, a passage through the two nanometer pores of the blood vessel endothelium in most healthy tissues or through the six nanometer gaps of postcapillary venules is prevented as liposomal carriers are characterized by a relatively large size of 45-150 nanometers [15]. However, during angiogenesis solid tumors develop a discontinuous endothelium characterized by large fenestrations allowing molecules to enter the interstitial space [19]. Moreover, once liposomes have entered the tumor tissue, they are retained from the malfunctioning lymphatic system and after its release the drug can exert its therapeutic effect [18, 19]. This phenomenon was termed the “tumor-selective enhanced permeability and retention (EPR) effect” or “passive tumor targeting effect” and has been studied in detail (see Fig. 4 and 5) [16, 17, 21]. Taken together, the therapeutic index of a cytostatic drug encapsulated in liposomes is increased by two main mechanisms: firstly, improved tolerability by a decrease in volume of distribution in the body and secondly, increased anti-tumoral efficacy by passive tumor targeting.

An excellent example for a successful clinical translation is liposomal doxorubicin, which improved the therapeutic index of doxorubicin while dose-limiting cardiotoxicity was significantly reduced [14, 19]. Approved formulations of liposomal doxorubicin (myocet™, caelyx™ and doxil™, lipo-dox™) are available for different tumor entities as Kaposi’s sarcoma, ovarian cancer, multiple myeloma as well as for metastatic breast cancer in Europe [22]. A significant reduction of nephrotoxicity has been demonstrated for a PEGylated liposomal formulation of cisplatin (lipoplatin™) which overcomes the significant risk of the dose-limiting adverse effect induced by conventional cisplatin [13]. Lipoplatin™ is currently evaluated for the treatment of non-small cell lung cancer in phase III trials and in 2007 it received “orphan drug” status as first line-treatment for pancreatic cancer in an ongoing Phase II/III trial [13, 23-25].

In the classical EDP-M regime, conventional formulations of the cytostatic drugs doxorubicin, cisplatin and etoposide are administered [9]. In recent years, it has been demonstrated that liposomal encapsulation of doxorubicin and cisplatin represents an important strategy to improve the properties of the parental drugs. Liposomal formulations of etoposide have not yet reached clinical trials status investigations. However, several preclinical *in vitro* and *in vivo* studies have revealed improved off-target profiles together with enhanced anti-tumoral efficacy [26].

### 1.3 Liposomal chemotherapeutic protocols as novel therapeutic approaches for ACC

In addition to the outlined general advantages of liposomally modified chemotherapies, in 2012 Hantel et al. were able to provide evidence for an extraordinary uptake phenomenon and internalization of liposomes specifically for adrenocortical cell lines (see Fig. 6) [27-29].

While the exact mechanism for this enhanced uptake of liposomes in adrenocortical tumor cells remains uncertain [27], this observation has clearly provided evidence for an additional potential role for liposomal chemotherapies in the treatment of ACC. Furthermore, the working group of Hantel et al. detected significant therapeutic efficacy of liposomal doxorubicin (caelyx™) in preclinical experiments utilizing a xenograft model for ACC [27].

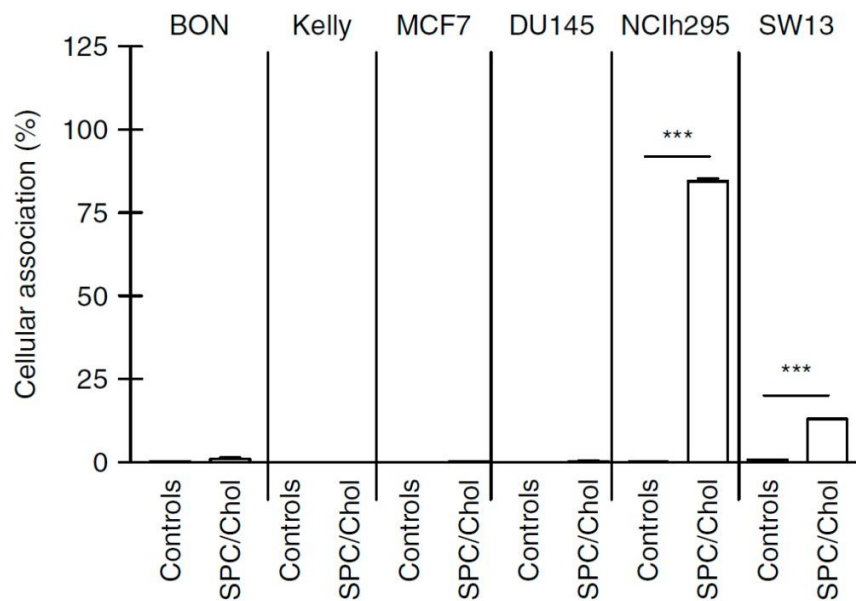


**Fig 6:** Cellular association of plain liposomes in different tumor cell lines BON (gastroenteropancreatic neuroendocrine tumors), Kelly (neuroblastoma), DU145 (prostate cancer), NCI-H295R and SW-13 (both models utilized for adrenocortical carcinoma) indicating a relevant uptake only in the adrenocortical cell lines (adapted from [27]). Stars denote significant differences; \*\*\*,  $p < 0.001$ .

Following these observations a liposomal variant of the classical EDP-M scheme referred to as “LEDP-M” was established [28]. This treatment scheme LEDP-M is composed of etoposide, liposomal doxorubicin, liposomal cisplatin and mitotane and was investigated in xenograft

models for ACC [28]. In this study, long-term experimental settings provided evidence for a sustained and highly significant anti-tumoral efficacy of LEDP-M compared to the classical EDP-M protocol (see Fig. 7).

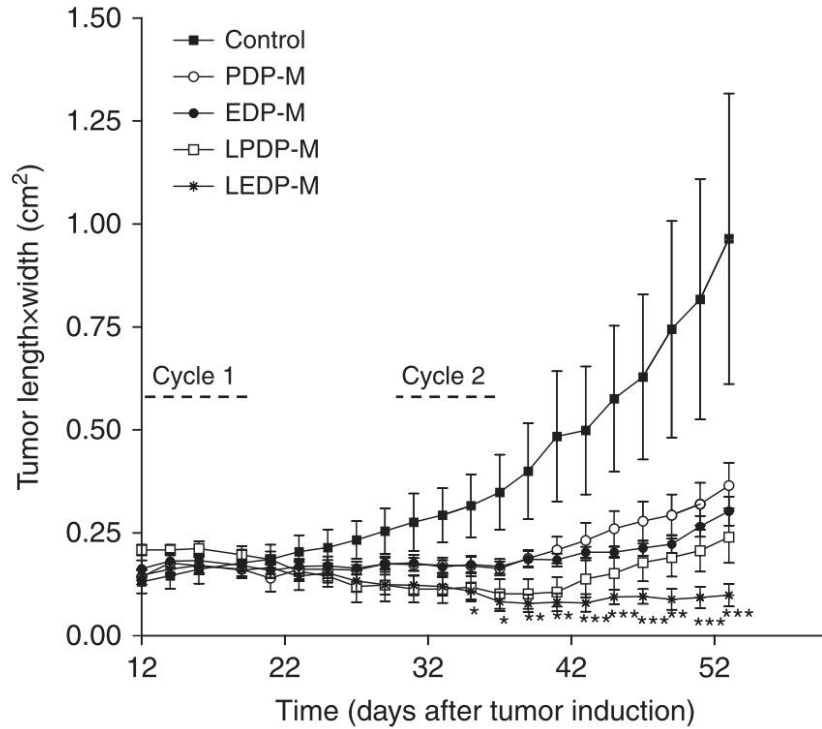


**Fig 7:** Tumor development in NCI-H295R tumor bearing mice upon different treatments including the therapeutic treatment protocols EDP-M and LEDP-M (adapted from [28]). In this experiment, also other therapeutic regimen PDP-M (cisplatin, doxorubicin, paclitaxel) and LPDP-M (liposomal cisplatin, liposomal doxorubicin, albumin-bound paclitaxel) were investigated. Stars depicted in the figure denote significant differences to EDP-M; \*,  $p < 0.05$ ; \*\*,  $p < 0.01$  and \*\*\*,  $p < 0.001$  [28].

The outcome and results of this preclinical study indicated that LEDP-M may represent an interesting option for the therapy of adrenocortical tumors [28]. Nevertheless, preclinical testing of novel therapeutic approaches for ACC is generally limited in clinical prediction as only one standardized xenograft model for ACC was available at the time.

#### 1.4 Human xenograft models of ACC

In addition to the development of novel therapeutic approaches appropriate preclinical tumor models are an essential and indispensable tool to proceed from preclinical testing to clinical trial status [30]. The situation is aggravated for ACC by the fact that the availability of human tumor models for ACC is very limited. Moreover, varied clinical presentation of patients with great differences in ACC biological behavior (for example high versus low or no functional activity) indicates the high heterogeneity of ACC [9, 10]. Consequently, this poses a major obstacle in finding appropriate and reliable preclinical *in vivo* models for ACC [30].

The most commonly used adrenocortical tumor model of human origin is NCI-H295R [30, 31]. This ACC cell line retained histological parameters compared with the original patient tumor from which the cell line was derived. NCI-H295R cells have furthermore shown to produce all major adrenal steroids [31]. NCI-H295R tumor cells can also be injected as subcutaneous tumor cell suspension in immunodeficient nude mice and a successful tumor development has been reported in about 90% of injected nude mice [32].

Another tumor model, SW-13, has been utilized in recent years for non-active ACC [33]. This tumor model contributed, for instance, to the demonstration of the importance of angiogenic pathways in ACC by studying the anti-tumoral effects of vascular endothelial growth factor receptor (VEGFR) tyrosine kinase inhibitors [34]. Furthermore, nanotechnologically modified albumin-bound paclitaxel was identified as a potential active substance for the treatment of ACC [35]. However, SW-13 does not originate from a primary adrenocortical carcinoma as it was established from a non-secreting small-cell carcinoma in the adrenal cortex [33]. Nevertheless, as other human tumor models for non-functional ACC were not available, SW-13 was widely accepted to be used for such studies in recent years.

Even though such cell line based tumor models can be utilized to establish tumor xenografts in immunodeficient mice, these tumors still originate from cell suspensions. Selection processes during high numbers of cell culture passages are very likely to lead to modified biologic properties and altered cell clone characteristics [30, 36]. Thus, resulting tumor xenografts might no longer reflect alterations in functional properties or specific therapeutic responses of the original patient tumor [36, 37]. In 2013, Pinto et al. established and characterized with SJ-ACC3 the first pediatric but also the first tissue-based tumor model for adrenocortical carcinoma [38]. Compared to the tumor models NCI-H295R and SW-13 which originate from cell lines, this

xenograft model is based on subcutaneous implantation of original patient tumor tissue. Originating from a pediatric patient tumor with endocrine functionality, the SJ-ACC3 xenograft model maintained the histopathologic and molecular features of the primary tumor [38]. Only recently, another successful re-implantation of cryoconserved SJ-ACC tumor pieces and subsequent therapeutic implementation of this tumor model was reported demonstrating its wide applicability in ACC research [39]. However, no cell line for complementing additional *in vitro* experiments could be established for SJ-ACC3 limiting the applicability of this tumor model.

Very recently, another patient-derived xenograft model, referred to as MUC-1, was established by subcutaneous implantation of a surgical tumor specimen. Moreover, also a human tumor cell line was established originating from MUC-1 xenografts [30, 39]. Consequently, the MUC-1 tumor model represents the only available human cell-line and tissue based xenograft model for ACC [30, 39] and is, thus, thought to further improve preclinical experiments in the future.

## 1.5 Circulating micro-RNAs as marker for therapeutic efficacy in ACC

Not only effective therapeutic strategies but also prognostic markers and indicators of treatment response are absolutely essential to improve the diagnosis and outcome of ACC therapy. Micro-RNA (miR) are defined as small non-coding RNA molecules which are important regulators for gene expression [40]. This characteristic feature promotes their role as important regulators for physiological, pathological settings and tumorigenesis [41]. Specific signatures of aberrant miR expression patterns have been demonstrated for a variety of malignancies including ACC [42, 43].

Novel findings have proven the existence of miR in body fluids as plasma samples and several circulating miR have been associated with different types of cancer [40]. Even if the source of circulating miR remains not fully understood [42], many miRs reveal similar expression changes in blood samples and tissues in various types of cancer [40, 43]. In accordance, correlations of circulating miRs in blood samples with cancer progression, therapy response and outcome of survival have been described [40, 43]. Such novel approaches provide evidence that miR have great potential to be used as minimal invasive biomarkers to monitor therapeutic responses upon anti-tumoral treatment [43]. In relation to ACC, plasma samples of patients have recently been analyzed for candidate miR as several miRs have been reported to be differentially expressed in adrenocortical adenoma or carcinoma tissues [42]. This study [42] revealed for miR-483-5p and miR-210, amongst others, elevated levels in plasma samples of ACC patients compared to adenoma samples.

MiR-483-5p represents one of the most investigated miR in adrenocortical tumors as it is transcribed from an intronic sequence of the insulin-like growth factor 2 (*IGF2*) gene [42]. This gene has been found to be overexpressed in ACC and was shown to significantly correlate with *IGF2* mRNA located in ACC tissue samples [42]. Moreover, elevated miR-483-5p expression has also been identified in a subgroup of patients with significantly poorer prognosis [43-45].

MiR-210 has been reported to be overexpressed in a variety of tumor entities including breast, lung and pancreatic cancer [46-49]. Several publications have revealed that hypoxia-inducible factor 1 $\alpha$  (HIF1 $\alpha$ ) is an important regulator for miR-210 expression [50]. HIF1 $\alpha$  represents an important regulatory factor overexpressed in a variety of tumors [50]. MiR-210 is referred to as the master hypoxamir and micromanager of the hypoxia pathway and is also known to be involved in cell cycle regulation, mitochondrial metabolism, DNA repair mechanisms and

angiogenesis [50, 51]. High miR-210 levels in ACC tumors have been furthermore shown to correlate with clinicopathological parameters of aggressiveness as well as poor prognosis [44]. Thus, intratumoral and especially circulating miR-210 and miR-483-5p levels represent interesting candidates for the development of novel ACC biomarkers.

## 1.6 General aim

Liposomal formulations of two out of three substances of the classical clinical EDP-M protocol are already in clinical use for other tumor entities highlighting the potential for a liposomal EDP-M regime. Thus, the development and application of liposomal chemotherapeutic regimens represent a promising innovative approach to develop novel treatment options for advanced adrenocortical tumors.

Therefore, the three main objectives of this project were:

1. The investigation of a classical EDP-M and the novel liposomal LEDP-M regimen in two xenograft models representing clinically relevant patient heterogeneity: SW-13 (hormonally inactive tumors) and SJ-ACC3 (pediatric tumors).
2. The establishment of a liposomal treatment scheme including also a liposomal formulation of etoposide (referred to as treatment arm L(I)EDP-M).
3. The investigation of intratumoral and circulating microRNA-210 and microRNA-453-5p levels upon therapeutic intervention to assess a putative applicability as therapeutic biomarkers for ACC.

## 2. Materials and Methods

### 2.1 Reagents and equipment

**Tab. 1:** General laboratory equipment

Material	Product specification	Company
Aqua distilled	7381901	Medizinische Klinik und Poliklinik IV, Munich, Germany
Bright-field microscope	DMRB	Leica Microsystems, Wetzlar, Germany
Bright-field microscope	Zeiss IM35	Carl Zeiss Microscopy GmbH, Oberkochen, Germany
Centrifuge Eppendorf	5415D	Eppendorf, Wesseling-Berzdorf, Germany
Centrifuge Hettrich	Ultra 2S	Hettrich, Tuttlingen, Germany
Ethanol	15091748	Medizinische Klinik und Poliklinik IV, Munich, Germany
Falcon Tubes (50 ml)	62547254	Sarstedt, Nümbrecht, Germany
Laboratory scale	BP 121 S	Sartorius, Göttingen, Germany
Laminar airflow bank	-	Heraeus, Hanau, Germany
Oven	Function Line	Heraeus, Hanau, Germany
Pipet tips (10-1000 µl)	701116200 70760211 70762200	Sarstedt, Nümbrecht, Germany
Pipets (10-1000 µl)	P10-P1000	Gilson, Villiers-le-Bel, France
Plate shaker mini rocker	L024	Kisker, Steinfurt, Germany
Safelock Eppendorf tubes	T9661, T2795	Sigma-Aldrich, Steinheim, Germany
Scale	EMB 220-1	Kern&Sohn, Balingen, Germany
Vortexer Vortex-Genie	SI-0136	Scientific Industries, Springfield, MA, USA

**Tab. 2:** Reagents and equipment for immunohistochemistry

<b>Material</b>	<b>Product specification</b>	<b>Company</b>
Acetic acid	137000	Merck-Millipore, Darmstadt, Germany
Bovine serum albumin	5482	Sigma-Aldrich, Steinheim, Germany
Citric acid	251275	Sigma-Aldrich, Steinheim, Germany
Cover glasses	48393-070	VWR GmbH, Darmstadt, Germany
DAB (3,3'-diaminobenzidine)	D4293	Sigma-Aldrich, Steinheim, Germany
DeadEnd Colorimetric TUNEL Kit	G7130	Promega GmbH, Mannheim, Germany
Embedding cassettes simport	M491-11 7-0010	Bernard-Pilon, Beloeil Quebec, Canada
Eosin Y solution	HT110232	Sigma-Aldrich, Steinheim, Germany
Goat serum	31876	Jackson Immuno Research, PA, USA
Hematoxylin Harris'	HHS32	Sigma-Aldrich, Steinheim, Germany
Hydrogen peroxide (H <sub>2</sub> O <sub>2</sub> )	107298	Merck-Millipore, Darmstadt, Germany
Ki67 primary antibody	KI68R06	DCS innovative diagnostics, Hamburg, Germany
Ki67 secondary goat anti- rabbit biotinylated IgG	BA-1000	Vector Laboratories, Burlingame, CA, USA
Liquid Blocker Super PapPen	MKP-1	Kisker, Steinfurt, Germany
Methanol	106009	Merck-Millipore, Darmstadt, Germany
Microtome	HM 355 E	Microm, Walldorf, Germany
Microwave	LCS1112SW	LG Electronics Deutschland GmbH, Ratingen, Germany
Paraffin	107337	Merck-Millipore, Darmstadt, Germany
Paraffin bath	SB 80	Microm, Walldorf, Germany
Paraformaldehyde (PFA)	P6148	Sigma-Aldrich, Steinheim, Germany
Permout mounting medium	SP15-500	Fisher Scientific, Fair Lawn, NJ, USA
Phosphate Buffered Saline (PBS) Pellets	P4417	Sigma-Aldrich, Steinheim, Germany

<b>Material</b>	<b>Product specification</b>	<b>Company</b>
Slides (superfrost plus)	J1800AMNZ	Menzel GmbH, Braunschweig, Germany
Sodium citrate	1613859	Sigma-Aldrich, St. Louis, MO, USA
Tissue processor	STP 120	Microm, Walldorf, Germany
Tween 20	P1379	Sigma-Aldrich, Steinheim, Germany
VectaMount AQ Mounting Medium	H-5501	Vector Laboratories, Burlingame, CA, USA
Vectastain Elite ABC Kit	PK-6100	Vector Laboratories, Burlingame, CA, USA
Vector Methyl Green	H-3402	Vector Laboratories, Burlingame, CA, USA
Xylene	108661	Merck-Millipore, Darmstadt, Germany

**Tab. 3:** Reagents and equipment for cell culture

<b>Material</b>	<b>Product specification</b>	<b>Company</b>
Cell culture flasks, 225 cm <sup>2</sup>	353138	Falcon, BD biosciences, Heidelberg, Germany
DMEM/F12	31330-095	Gibco Invitrogen, Darmstadt, Germany
Dulbecco's Phosphate Buffered Saline (PBS) sterile	14190-094	Gibco Invitrogen, Darmstadt, Germany
Fetal bovine serum (FBS)	10500064	Gibco Invitrogen, Darmstadt, Germany
Incubator	Hera cell 150	Heraeus, Hanau, Germany
Insulin-Transferrin-Selenium supplement	41400-045	Gibco Invitrogen, Darmstadt, Germany
Medium 199	2350-029	Gibco Invitrogen, Darmstadt, Germany
Neubauer counting chamber (Neubauer improved)	0,0025 mm <sup>2</sup> , 0,100 mm	PEQLAB Biotechnologie GmbH, Erlangen, Germany
Penicillin/Streptomycin (P/S)	15140-122	Gibco Invitrogen, Darmstadt, Germany
Trypan blue solution	15250-061	Gibco Invitrogen, Darmstadt, Germany
Trypsin-EDTA 0,05%	25300-054	Gibco Invitrogen, Darmstadt, Germany
UltrosorG	15950-017	CytoGen GmbH, Sinn, Germany

**Tab. 4:** Reagents and equipment for animal experiments

Material	Product specification	Company
Animals (female, 6–8 weeks old)	Athymic NMRI <i>nu/nu</i> mice	Harlan Winkelmann, Borchon, Germany
Antisedan (Alzane)	45655R-0512	Pfizer GmbH, Berlin, Germany
Domitor (Dorbene)	45081R-0313	Pfizer GmbH, Berlin, Germany
Isoflurane (Forene)	05260-05	Abbott GmbH, Wiesbaden, Germany
Isoflurane vaporizer	UnivetPorta Narkosesystem	Groppler Medizintechnik, Düsseldorf, Germany
Isopropanol	100995	Merck-Millipore, Darmstadt, Germany
Ketamin (Ketavet)	PZN 7506004	Pfizer GmbH, Berlin, Germany
Microvettes (EDTA)	200K3E	Sarstedt, Nürmbrecht, Germany
Novalgin (Novalminsulfon)	N95362.14	Ratiopharm GmbH, Ulm, Germany
Permanent marker	3000	Edding Vertrieb GmbH, Wunstorf, Germany
Protective clothing	-	Zentrale Versuchstierhaltung, Kliniken Innenstadt, Munich, Germany
Restrainer	Type Broome HAR- 52-04	Föhr Medical Instruments GmbH, Seeheim/Ober-Beerbach, Germany
Scalpel	0200130010	PFM medical AG, Cologne, Germany
Sodium chloride 0,9% (NaCl) sterile	5122110950411	Braun AG, Melsungen, Germany
Surgical equipment (forceps, scissors, thread holder)	HSB 391-10 HSC 011-04 HWC-075-13 HSE-028-142	Hammacher, Solingen, Germany
Surgical suture material	Prolene EH7289H	Ethicon, Somerville, NJ, USA
Syringes BD Microfine (U40, 0.5 and 1 ml)	324876 320801	Becton Dickinson, Heidelberg, Germany

**Tab. 5:** Therapeutic substances and solutions

<b>Material</b>	<b>Product specification</b>	<b>Company</b>
Caelyx™ (PEGylated liposomal doxorubicin)	PZN 07683692	Janssen-Cilag GmbH, Neuss, Germany
Cisplatin	local pharmacy	Klinikum der Universität München, Apotheke Campus Großhadern, Munich, Germany
Corn oil	C8267	Sigma-Aldrich, Steinheim, Germany
Doxorubicin	local pharmacy	Klinikum der Universität München, Apotheke Großhadern, Munich, Germany
Etoposide	local pharmacy	Klinikum der Universität München, Apotheke Campus Großhadern, Munich, Germany
Lipoplatin™ (Liposomal Cisplatin)	Provided by Regulon Inc.	Regulon Inc., Athens, Greece
Liposomal Etoposide	CM-EL-02L-Alpha-Phosphatidylcholine 76.5 mM Cholesterol 56.1 mM 1,2-distearoyl-sn-glycero-3-phosphoethanolamine-N-[methoxy(polyethylene glycol)-750] 6.99 mM Etoposide 8.49 mM 0.01 M Phosphate buffered Saline; 0.138 M NaCl, 0.0027 M KCL (pH 7.4)	Encapsula NanoSciences, TN, USA
Mitotane	25925-1GF	Sigma-Aldrich, Steinheim, Germany

**Tab. 6:** Reagents and equipment for molecular analysis

Material	Product specification	Company
Fast-Real-Time PCR System 7500	4351105	Applied Biosystems, CA, USA
MiRNeasy mini kit	217004	Quiagen, CA, USA
NanoDrop spectrophotometer	2000	ThermoFisher Scientific, MA, USA
Proflex Base PCR System	4484076	ThermoFisher Scientific, MA, USA
Spike-in control miR cel-miR-39	2594091	Quiagen, CA, USA
TaqMan Fast Universal PCR Master Mix	4304437	Applied Biosystems, CA, USA
TaqMan microRNA reverse transcription kit	4366596	Applied Biosystems, CA, USA,
TaqMan miRNA assays	Hsa-miR-210 (#000512), Hsa-miR-483-5p (#002338), RNU44 (#001094), cel-mir-39 (#000200)	Applied Biosystems, CA, USA
Total Exosome Isolation Kit	4484450	ThermoFisher Scientific, MA, USA
Total Exosome RNA and Protein Isolation Kit	4478545	ThermoFisher Scientific, MA, USA

**Tab. 7:** Solutions and their preparation protocols

Solution	Ingredients
0.3% hydrogen peroxide in methanol	hydrogen peroxide 30% 500 µl
	methanol 50 ml
4% paraformaldehyde (PFA)	paraformaldehyde 20 g
	distilled water 450 ml
	10X PBS 50 ml
	1M NaOH
	1M HCl
	goat serum 5 µl
<p>Preparation protocol: 450 ml of distilled water are placed in a glass beaker and heated to 60°C. While the mixture is stirring, 20 g of paraformaldehyde powder are added to the hot water, the glass is covered and maintained at 60°C. Thereafter, five drops of NaOH are added and the solution clears within minutes. The solution must not be heated above 70°C. After receiving a clear solution, the glass baker is removed from heat and 50 ml of 10X PBS are added. The pH should be adjusted to a pH of 7.2 and the solution filled up to a final volume of 500 ml. Finally, the solution is filtered, placed on ice and protected from light.</p>	
Acid ethanol	50 ml 70% EtOH
	0.125 ml concentrated HCl
Sodium citrate buffer	0.1M citric acid solution 21 g / 1000 ml (A)
	0.1M sodium citrate 29 g / 1000 ml (B)
	buffer solution: 9 ml solution A + 41 ml solution B
Tap water substitute	1 g NaHCO <sub>3</sub>
	10 g MgSO <sub>4</sub> *7H <sub>2</sub> O
	fill with distilled water up to 500 ml

**Tab. 8:** Software

<b>Software</b>	<b>Specification</b>
Microsoft Excel 2010	Microsoft Corporation 2010, NM, USA
Microsoft Office PowerPoint 2010	Microsoft Corporation 2010, NM, USA
SPSS statistics 23	Ehningen, Germany
Prism Software 3.02	Houston, TX, USA
ImageJ 1,5b	National Institute of Health (NIH), MD, USA

## 2.2 Cell culture and tumor cell preparation for tumor induction

SW-13 cells were obtained from ATCC and recently authenticated. Adherent cells were cultured at 37°C providing a 5% CO<sub>2</sub> - 95% air atmosphere. Cells were maintained in culture for at least two weeks before tumor induction was performed.

DMEM/F-12 cell culture medium was used which was supplemented with penicillin/streptomycin (1%) and heat inactivated fetal bovine serum (10%, see Tab. 3). Cells were split every 3-4 days in a ratio of 1:8 – 1:10. Cell culture flasks were used in 75 cm<sup>2</sup> or 225 cm<sup>2</sup> size.

For xenograft induction, tumor cells were subcutaneously injected into the neck of individual animals. For this purpose, tumor cells were grown in 225 cm<sup>2</sup> flasks for cell culture. At the day of tumor cell injection, four 225 cm<sup>2</sup> cell flasks were processed at the same time. After washing with PBS, 5 ml trypsin was added to every flask and kept at 37°C to achieve complete separation of tumor cells. The trypsin reaction was terminated by the addition of 18 ml cell culture medium and cell suspension was filled in two 50 ml falcon tubes. After a centrifugation step for 5 minutes, all cell pellets were dissolved in 15 ml PBS. The whole procedure was repeated with four additional 225 cm<sup>2</sup> cell flasks to receive a total volume of 30 ml cell suspension. The suspension was carefully mixed and cells were counted using a Neubauer counting chamber (see Tab. 3).

For the counting procedure, 1 ml of cell suspension was placed into a new falcon and mixed with 9 ml PBS (dilution 1:10). 10 µl of this diluted cell suspension were then mixed with trypan blue solution (1:4) and the number of viable cells was determined using the microscope. Afterwards, the cell number per ml and total cell number were calculated. After the determination of the exact volume which contained the desired cell number for tumor cell injection, the cell suspension was diluted to a final injection volume of 200 µl, drawn into 1 ml syringes and immediately injected into the neck of the individual mice (see 2.3.2).

## 2.3 Animal experiments

### 2.3.1 Housing conditions

All animal studies were approved by the Regierung von Oberbayern and in accordance with regulations of the German guidelines for animal experiments. NMRI *nu/nu* mice (female athymic, 6–8 weeks old) were obtained from Harlan Winkelmann GmbH and kept under pathogen-free conditions at an ambient temperature of  $22 \pm 2^\circ\text{C}$  on a 12 hour light-dark cycle. Access to standard diet and drinking water was granted ad libitum. Handling of the animals was performed under a sterile airflow chamber using protection clothes, gloves and a surgical mask. The mice were kept in the animal house at least one week before starting the experiments.

### 2.3.2 Preclinical tumor models and tumor induction

Preclinical tumor models were based on subcutaneous tumor cell injection or implantation. Two different xenograft models for ACC (SW-13 and SJ-ACC3) were implemented in this study. Their characteristics are illustrated compared to the classical NCI-H295 tumor model in Fig. 8.

Tumor xenograft model	Tumor induction	Detectable solid tumor	Tumor diameter of 1.5 cm
 SW-13	Cell injection $11\text{-}13 \times 10^6$	~ 4 days	> 40 days
 SJ-ACC3	Cryoconserved $2 \times 2 \times 2 \text{ mm}^3$ tumor pieces	~ 1 month	> 90 days
 NCI-H295R	Cell injection $15 \times 10^6$	~ 10 days	> 20-30 days

**Fig. 8:** Overview and characteristics of SW-13, SJ-ACC3 and classical NCI-H295 xenograft tumor models

### 2.3.2.1 Cell-line based SW-13 tumor model

Tumor induction for SW-13 and NCI-H295 xenografts was performed by a subcutaneous injection of tumor cells into the neck of individual mice. To achieve an accurate and reproducible tumor cell injection, isoflurane anesthesia was applied (6 l/min flow-rate and 5% isoflurane concentration). Tumor cells were prepared according to 2.2. For SW13-xenografts,  $13 \times 10^6$  and  $11 \times 10^6$  tumor cells per mouse were injected in short-term and long-term experiments, respectively.

### 2.3.2.2 Xenograft based SJ-ACC3 tumor model

For SJ-ACC3 xenografts [38], cryopreserved tumor specimens of 2 mm<sup>3</sup> size were subcutaneously implanted. Tumor pieces were transferred prior implantation from liquid nitrogen to a 37°C water bath and rinsed several times in medium 199 supplemented with 1% penicillin/streptomycin. Afterwards, tumor tissue was kept in medium 199 until implantation.

For the implantation procedure, animals received pre- and postsurgical analgesia and were anesthetized according to Table 9.

**Tab. 9:** Doses and application routes regarding anesthesia and analgesia for tumor implantation

Drug	Novalgine	Domitor	Ketavet	Antisedan
<b>Injection</b>	s.c.	i.p.	i.p.	i.m.
<b>Dosage (mg/kg mouse)</b>	200	0.3	60	1.5
<b>Concentration drug (mg/ml)</b>	500	1	100	5
<b>Dilution (0.9% NaCl)</b>	1:10	1:10	1:20	1:10
<b>Injected diluted substance in <math>\mu</math>l per g mouse</b>	4	3	12	3

Novalgine was administered in a 12 hour rhythm post-surgery to achieve a sustained analgesia. Using surgical scissors and forceps, a 3-4 mm cut was induced into the neck of individual animals and the skin was carefully lifted to have access to a subcutaneous cavity where the tumor piece was placed. For tumor pieces an individual forceps was used. Afterwards, the cut was surgically sutured and anesthesia was antagonized with antisedan. Animals were put for the wake-up procedure in individual cages and warmed with infrared light.

### **2.3.3 Therapeutic experiments**

Therapeutic experiments were performed in two different settings with short-term and long-term duration. For SW-13, short-term experiments were started at day 14 (n=7-8 mice) and long-term experiments at day 4 (n=14 mice) after tumor cell injection. For SJ-ACC3, short-term and long-term therapeutic treatment was started after several weeks (n=4-6 mice). Only mice bearing successfully engrafted tumors were included in subsequent therapeutic experiments.

#### **2.3.3.1 Preparation of therapeutic drugs**

For therapeutic experiments, a preclinically adapted scheme of the classical EDP-M (Berruti) protocol [9, 52] was administered as already implemented in a recent study [28] (Fig. 11). The administration of all therapeutic treatments was performed in 24 hour intervals.

Mitotane powder was stored in the refrigerator at 4-6°C until use and protected from light. Corn oil was autoclaved in small aliquots and used for dissolving mitotane powder at room temperature. After the autoclaving procedure, only clear corn oil was used. 500 mg mitotane powder were dissolved in 10 ml corn oil to achieve a final concentration of 50 mg/ml. As the powder was very poorly soluble, the corn oil had to be added carefully and mixed well for about 10 minutes. Dissolved mitotane was filled into a falcon tube and protected from light. The appropriate volume for each animal was calculated and slowly drawn into 1 ml syringes (Tab. 4).

Dissolved mitotane was intraperitoneally injected applying a daily dose of 300 mg/kg body weight over three consecutive days prior cytostatic treatment. Control animals were treated with appropriate volumes of autoclaved corn oil. If necessary, cytostatic drugs were dissolved in sterile 0.9% sodium chloride on the day of injection and intravenously applied in a 2 mg/kg dose

of cisplatin and lipoplatin™ as well as 10 mg/kg doses of doxorubicin, liposomal doxorubicin (caelyx™), etoposide and liposomal etoposide according to the treatment modalities outlined for one therapeutic cycle (Fig. 11). For intravenous injections, animals were immobilized with a mouse restrainer and their tails were warmed up using infrared light to facilitate the injection procedure.

### 2.3.3.2 Therapeutic treatments and sample collection

In short-term experiments, tumor bearing mice were treated with one therapeutic cycle according to the treatment regime illustrated in Fig. 9 and 10, respectively. 48 hours after the last therapeutic intervention these studies were terminated and animals euthanized. After isoflurane anesthesia, animals were sacrificed and EDTA blood was collected and put on ice. Afterwards the tumors were excised and processed for paraffin embedding by immersion in 4% PFA overnight at 4°C. In case of sufficient material tumors were also snap-frozen in liquid nitrogen. EDTA-blood was centrifuged at 2000 G-force and 4°C to obtain plasma samples. Furthermore, 100 µl of whole blood was collected in EDTA-microvettes to enable an analysis of leukocytes. Frozen tumor and plasma samples were kept at -80°C until further analysis was performed.

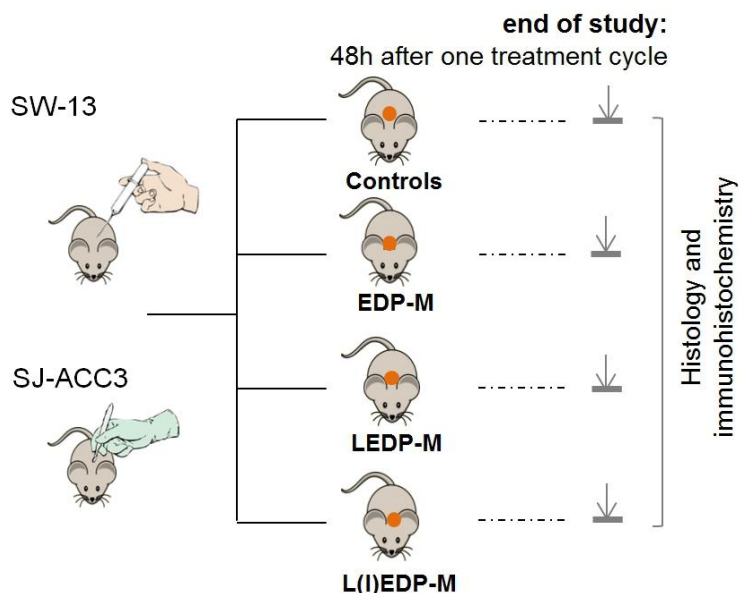


**Fig. 9:** Therapeutic setting in the short-term study. Following one therapeutic cycle, tumor tissues of controls, EDP-M, LEDP-M and L(I)EDP-M were investigated using histology and immunohistochemistry.

In long-term therapeutic experiments individual mice received repeated treatment cycles with a therapy-free interval of ten days between the treatment cycles. During these studies, the animals were monitored every day and tumor sizes were measured every second day (as tumor length x width [cm<sup>2</sup>]).

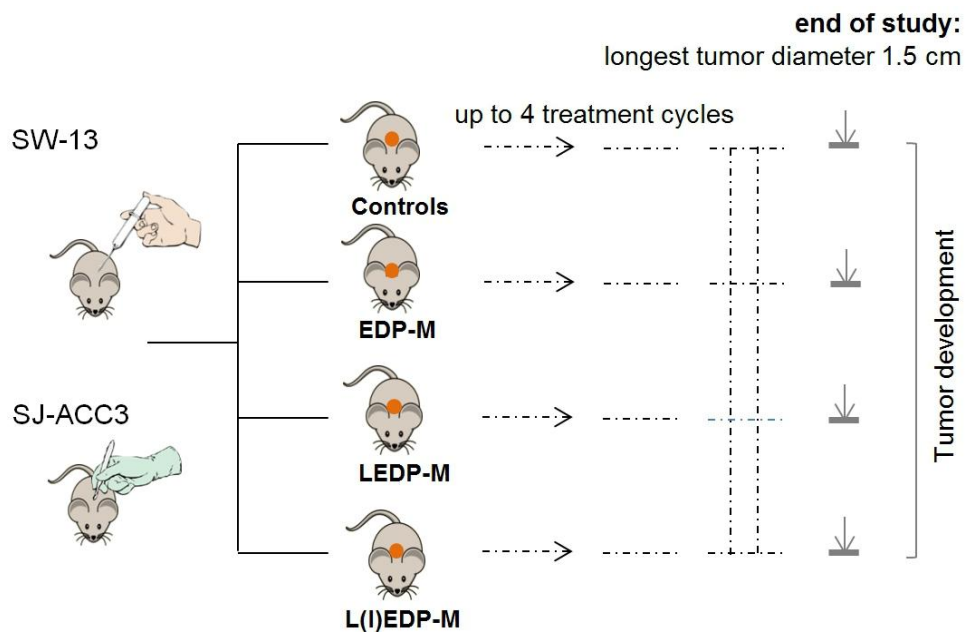


**Fig. 10:** Therapeutic setting for long-term experiments with monitoring of individual tumor development in the different therapeutic groups EDP-M, LEDP-M, L(I)EDP-M and controls.

Tumor growth curves were analyzed for both tumor-models at least upon administration of two therapeutic cycles. While for SJ-ACC3 the long-term study was terminated afterwards, SW-13 tumor bearing mice were treated with up to four therapeutic cycles to allow a more detailed investigation of overall survival and off target profiles of the different treatment modalities (see Fig. 10). In this setting mice were sacrificed when tumors reached a longest pre-defined tumor diameter of 1.5 cm or when specified side-effects effects (body weight loss or pathologically changed phenotype as abnormal body posture) occurred.

For additional immunohistochemical and histological analysis also hearts and kidneys were snap-frozen and paraffin-embedded to enable a more detailed investigation as these organs represent the main off-target organs of cytostatic treatment with doxorubicin and cisplatin, respectively.

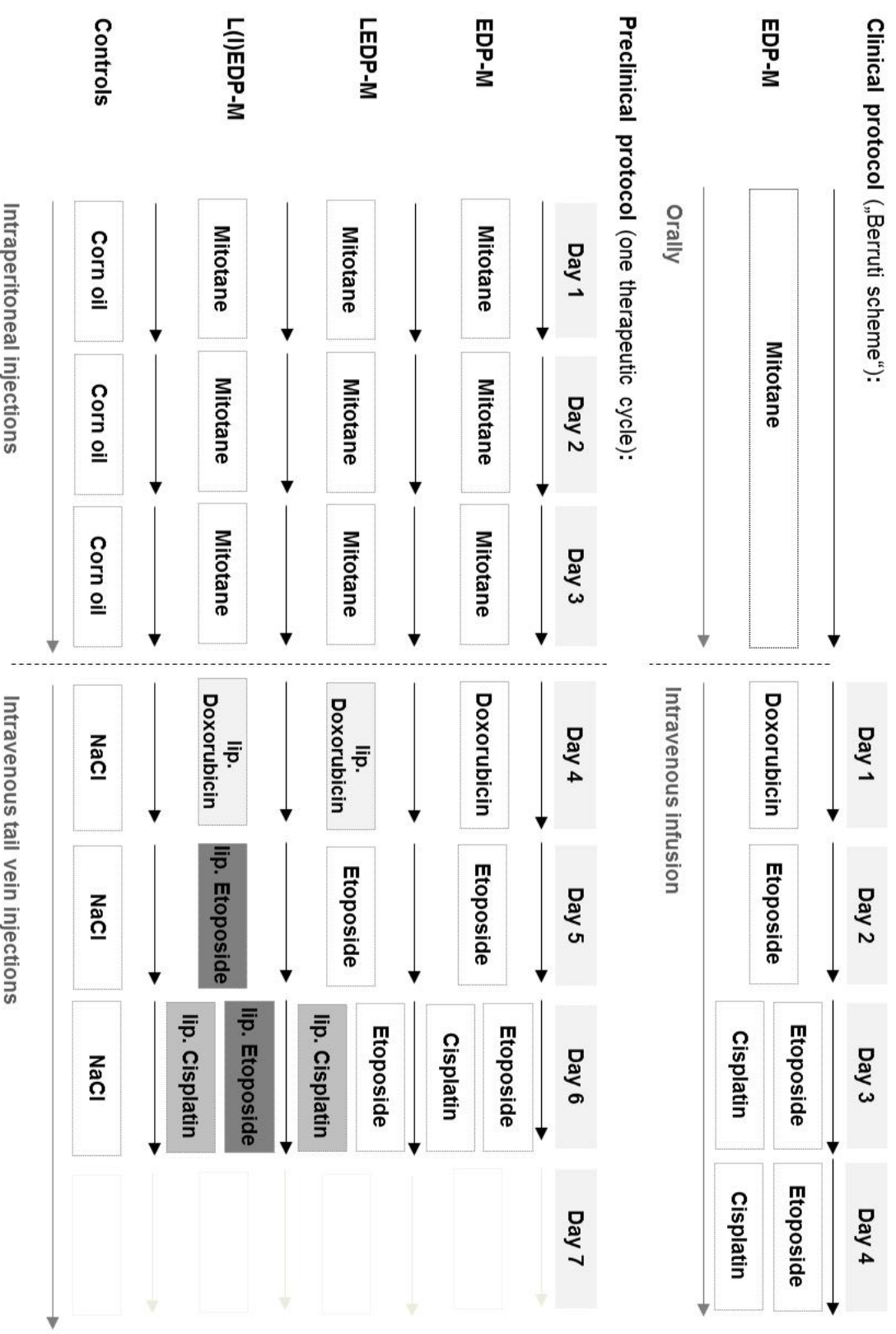


**Fig. 11:** Schematic illustration of the preclinical treatment schemes adapted from the clinical EDP-M (Berruti) protocol. Treatment protocols are illustrated for one therapeutic cycle including intraperitoneal and intravenous injections (adapted from [28]).

### **2.3.4 Histology and immunohistochemistry**

Tumor tissue, kidneys and hearts were after collection embedded in paraffin and subsequently processed and prepared for immunohistochemistry or histology. If not stated otherwise, all procedures were performed at room temperature.

#### **2.3.4.1 Paraffin embedding of tissues**

Tumor tissues, kidneys and hearts from sacrificed mice were immediately placed in a 4% PFA solution and kept overnight at 4°C on a shaker to enable an appropriate fixation of tissues. For each tissue, at least 10 ml PFA were used. Afterwards, tissues were immersed and dehydrated in 30%, 50% and 70% ethanol for two hours each. The following steps were performed in an automatic tissue processor (see also Tab. 2). Incubation in 96% ethanol (2 x 2 h) was followed by immersion in 100% ethanol (3 x 2 h). After these ethanol immersion steps tissue was further processed in xylene (2 x 2 h) and liquid paraffin (2 h and 7 h). Embedding in paraffin was performed at a paraffin temperature of 60°C using a tissue processor machine (Tab. 2). Paraffin blocks containing the tissue samples were stored at room temperature and were protected from light until further analysis.

#### **2.3.4.2 Preparation of tissue for immunohistochemistry and histology**

Paraffin embedded tissues were cut with a microtome in 4 µm sections. A paraffin bath set on 40-45°C was used to achieve flattening of the tissue section. To promote an efficient drainage, slides were vertically removed from the bath and excess water was blotted using a paper tissue. Afterwards, sections were dried on glass slides overnight in an incubator at 37°C.

For histological and immunohistochemical stainings, tissue sections were incubated in xylene (2 x 6 min.) followed by an immersion in 100% ethanol (2 x 6 min.), 96% ethanol (2 x 6 min.) and 70% ethanol (1 x 6 min.). Afterwards, sections were put in distilled water and were further processed according to the individual staining protocols.

### **2.3.4.3 Immunohistological and histological evaluation**

In general, tumors were immunohistochemically evaluated investigating six high power fields (HPF, 0.391 mm<sup>2</sup>, 400x magnification) per tumor [28, 53] and histologically screened for necrosis. Kidneys and hearts were also investigated for pathological alterations. Assessment of cardiotoxic effects and pathological evaluation was performed in cooperation with the Institute of Pathology in Munich (Dr. Max Weiss).

### **2.3.4.4 Ki67 immunohistochemistry**

For Ki67 immunohistochemistry, rehydrated sections were immersed in distilled water. 10 mM sodium citrate buffer was used to achieve efficient antigen retrieval. The slides were put into pre-warmed citrate buffer, were boiled for 15 minutes in the microwave and cooled down at room temperature for one hour. The slides were then immersed for 10 minutes in 0.3% H<sub>2</sub>O<sub>2</sub> in methanol to perform peroxidase blocking which avoids non-specific staining. After subsequent washing steps in PBS (2 x 5 min.) the slides were incubated in blocking buffer containing 3 % BSA, 5 % goat serum and 0.5 % Tween 20 for 15 minutes. Afterwards, primary Ki67 antibody (1:200 in blocking buffer) was applied which specifically stains proliferating cells.

Following overnight incubation at 4°C, slides were three times rinsed for 5 minutes in PBS. Tissue was covered with secondary polyclonal antibody (1:200 in blocking buffer) at room temperature for 30 minutes. After immersion in PBS (3 x 5 min.), Vectastain ABC Kit was applied according to the manufacturer's protocol (Table 2): 100 µl blocking solution, 1 µl reagent A and 1 µl reagent B were combined 30 minutes before use and this solution was then applied to the tissue. Afterwards, washing steps in PBS (3 x 5 min.) were performed and primary antibody was visualized by incubating the tissue in 3,3'-diaminobenzidine (DAB) for 3 minutes. For counterstaining, Vector®methyl green nuclear counterstain was applied for 10 minutes at 60°C to enable cell number quantification of Ki67 positive and negative cells. The slides were very quickly dehydrated in 30 sec. 96% ethanol and this step was repeated. Finally, the tissue was repeatedly immersed for 30 sec. 100% ethanol and in xylene for 2 x 5 minutes. Permount mounting medium was applied to cover the slides which were afterwards dried for 24 hours over night.

#### **2.3.4.5 TUNEL immunohistochemistry**

Apoptotic cells were visualized using the colorimetric DeadEND™ TUNEL System which measures the nuclear DNA fragmentation to detect apoptotic cells (see also Tab. 2).

According to the manufacturer's protocol, tissue sections were deparaffinized and rehydrated. Subsequent incubation with Proteinase K solution was performed for 10 minutes. The reaction mix was prepared as described in the protocol. During incubation with the reaction mix, biotinylated nucleotide is incorporated at the 3'-OH DNA supported by an enzyme referred as "Terminal Deoxynucleotidyl Transferase (Recombinant)" (for further information see Tab. 2). As described in the manual, the reaction was stopped after one hour and after several washing steps blocking of endogenous peroxidases was carried out with 0.3 % hydrogen peroxide. After washing steps, streptavidin horseradish peroxidase incubation was performed to bind horseradish peroxidase-labeled streptavidin to biotinylated nucleotides. In a last step, peroxidase substrate, hydrogen peroxide and diaminobenzidine were combined. Tissue samples were incubated in this mixture for 10 minutes to achieve a dark brown staining of apoptotic cells. 70 µl of VectaMount AQ Mounting were applied at each tissue and the slides were covered using cover slips and dried for 24 hours. Immunohistological evaluation was performed using a bright field microscope (see Tab. 1).

#### **2.3.4.6 Hematoxylin/Eosin staining**

Histological evaluation of kidney and heart sections was performed using regressive hematoxylin/eosin staining. Tissue was deparaffinized by repeatedly immersing the slides for 5 min. in xylene, followed by 3 x 3 minutes washing steps in 100% ethanol and 3 min. in 96% and 80% ethanol. Afterwards, the slides were immersed for five minutes in distilled water. While the sections were immersed in the water, the surface of hematoxylin was skimmed with a wipe to remove oxidized particles. Excess water from the slide and slide holder was blotted before the slides were incubated for 2.5 minutes in hematoxylin. Tap water substitute (Tab. 7) was used to blue the stainings for 5 minutes. After staining with hematoxylin, the slides were ten times dipped into acid ethanol for de-staining and immersed for 2 x 1 min. in tap water substitute followed by washing steps in distilled water. Excess water was blotted from the slides before immersion into eosin for 45 seconds. Slides were immediately put into 95% ethanol for 2 x 5 min. and 100%

ethanol for 2 x 5 minutes. Excess ethanol was blotted before going into final xylene dehydration steps for 2 x 10 min. and afterwards the slides were covered using permount mounting medium.

## **2.4 Molecular Analyses**

For micro-RNA (miR) analysis with quantitative real-time PCR (RT-qPCR), SW-13 and SJ-ACC3 tumor specimens and plasma samples of the short-term experiments were processed to isolate the total RNA of each sample (different kits and equipment see Tab. 6).

Tumor tissue was pulverized in liquid nitrogen and processed according to the instructions in the miRNeasy mini kit which is designed to purify total RNA including miR and other small RNA molecules. After the isolation procedure, 30  $\mu$ l RNA in distilled water were obtained.

According to the manufacturer's total exosome isolation and total exosome RNA and protein isolation kit, isolation of circulating RNA from plasma exosomes was performed by processing the plasma samples. Exosomes are defined as small vesicles which are secreted by all types of cultured cells, contain nucleic acid and proteins and are released to extracellular fluids in exocytic bursts by fusion with the cell surface (see also in the manufacturer's protocol, Tab. 6). Before Acid-Phenol Chloroform extraction, spike-in control miR cel-miR-39 was added and then total RNA isolation was proceeded as described in the manual's instructions. Finally, the concentration of RNA was determined using NanoDrop 2000 spectrophotometer and RNA samples were stored at -80°C until use. If necessary, total RNA was diluted to a concentration of 2 ng/ $\mu$ l and reverse transcribed using specific TaqMan MicroRNA Reverse transcription kit on Proflex Base PCR System.

For reverse transcription, reactions were run in a total volume of 7  $\mu$ l master mix, 3  $\mu$ l primer and 5  $\mu$ l RNA sample as described in the manufacturer's protocol. Quantitative RT-PCR was performed using a 7500 Fast-Real-Time PCR System with TaqMan Fast Universal PCR Master Mix (2x) and TaqMan miRNA assays. The reaction was performed in a total volume of 15  $\mu$ l containing 6.1  $\mu$ l nuclease-free water, 7.5  $\mu$ l Taqman Fast Universal PCR Master Mix, 0.5  $\mu$ l TaqMan miR assays and 0.9  $\mu$ l reverse transcription product. Reactions were run in duplicates on a 96-well plate.

Human primer assays were as follows: Hsa-miR-210 (#000512) and hsa-miR-483-5p (#002338) (Tab. 6). For tumor samples RNU44 (#001094) and for plasma samples cel-mir-39 (#000200) were used as housekeeping genes [40, 54].

For the evaluation of changes in miR level upon therapy with NaCl or LEDP-M in each mouse, the ratio of intratumoral to circulating miR level was calculated (referred to as “miR ratio”) after normalization to controls (% of controls) [53]:

$$\frac{\text{intratumoral miR [\%]}}{\text{circulating miR [\%]}} = \text{miR ratio (individual animal)}$$

A value of 1 indicates unchanged levels in tumor and plasma. Accordingly, a value of >1 reveals an elevated expression of intratumoral miR while a ratio of <1 indicates elevated expression of circulating miR [53].

## 2.5 Clinical experiments

Six patients with very advanced ACC that have benefited in the past from EDP-M were offered liposomal doxorubicin or liposomal cisplatin (referred here as liposomal EDP-M, lipEDP-M) on a compassionate-use basis (see Tab. 1). All patients had experienced toxicity upon classical EDP-M treatment and/or desired experimental therapy.

All study participants were informed by the experimental nature of this drug administration and gave informed consent in verbal and written form. Following criteria were evaluated: 1. reason for liposomal EDP-M, 2. change in sum of target lesions, 3. best objective response, 4. serious side-effects, 5. kidney function (using the MDRD formula ml/min/1.73 m<sup>2</sup>) and 6. individual patient's evaluation of liposomal EDP-M protocol. Patient recruitment, collection and evaluation of data were performed in a cooperation project, managed by Prof. Dr. med. Fassnacht-Capeller (Wuerzburg) and Prof. Dr. med. Felix Beuschlein (Munich).

## 2.6 Statistical analysis

Data are presented as mean ± standard error of the mean (SEM). For statistical analysis, Prism Software 3.02 (Houston, TX, USA) or SPSS statistics 23 were utilized. After analysis of normality distribution, One-way ANOVA (analysis of variance) followed by Bonferroni's Multiple Comparison Test (comparing all treatment groups) or unpaired t-test was applied. Both tests included an adjustment of 95% confidence interval (CI). For analysis of survival, log-rank (Mantel Cox) test was utilized. Statistical significance is defined as p<0.05 and indicated as asterisk (\*, p<0.05; \*\*, p<0.01; \*\*\*, p<0.001) in the figures if not stated otherwise.

### **3. Results**

Tumor bearing animals were treated according to the treatment schemes for short-term or long-term experiments (see 2.3.3.2). For short-term experiments, tumors were investigated by histology and immunohistochemistry. Blood samples were analyzed for leukocyte count. In long-term experiments, tumor development and off-target profiles were assessed.

#### **3.1 Short-term therapeutic efficacy**

Anti-tumoral efficacy of EDP-M, LEDP-M and L(I)EDP-M was investigated in SW-13 and SJ-ACC3 tumors after administration of one therapeutic cycle (see Fig. 11). Experimental setting, therapeutic regimens and treatment groups are described in 2.3.3. 48 hours after the last therapeutic intervention animals were euthanized. Blood samples were collected and SW-13 and SJ-ACC3 tumor tissues were investigated for tumor cell proliferation by Ki67 immunohistochemistry. Furthermore, induction of apoptosis was analyzed by TUNEL immunohistochemistry and tumors were histologically evaluated utilizing hematoxylin/eosin staining (see 2.3.4).

##### **3.1.1 Evaluation of the total number of tumor cells**

For both xenografts models, highest total number of tumor cells (Ki67-positive and negative fraction [cells/high-power field/tumor]) was, as expected, detected in the control groups (SW-13:  $28.9 \pm 2.2$ , Fig. 12A; SJ-ACC3:  $35.9 \pm 1.3$ ; Fig. 13A).

While all treatments showed anti-proliferative effects against SW-13 revealing highest efficacy upon L(I)EDP-M administration (EDP-M:  $20.5 \pm 1.6$ ,  $p < 0.01$ ; LEDP-M  $17.2 \pm 1.3$   $p < 0.001$  and L(I)EDP-M  $14.7 \pm 0.9$ ,  $p < 0.001$ , versus controls; Fig. 12A), for SJ-ACC3 only EDP-M induced a significant reduction in the number of tumor cells compared with controls (EDP-M:  $30.3 \pm 1.2$ ,  $p < 0.05$ ; LEDP-M  $31.5 \pm 1.8$ ,  $p > 0.05$  and L(I)EDP-M  $32.5 \pm 0.3$ ,  $p > 0.05$  versus controls; see Fig. 13A).

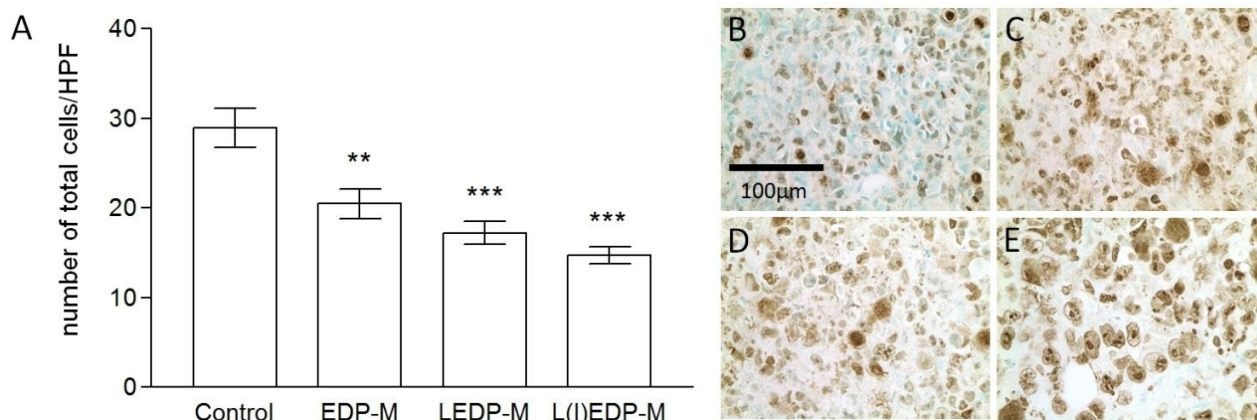


**Fig. 12:** Immunohistochemical analysis of SW-13 tumor tissues derived from the short-term therapeutic study. The quantification of the total number of tumor cells per HPF (Ki67-positive and Ki67-negative cells) is illustrated in (A). Representative pictures are presented for NaCl (B), EDP-M (C), LEDP-M (D) and L(I)EDP-M (E) treated tumors. Statistical significance versus controls is indicated with asterisks (\*,  $p < 0.05$ ; \*\*,  $p < 0.01$ ; \*\*\*,  $p < 0.001$ ).

For SW-13, the detected decrease in the number of tumor cells was furthermore accompanied by a severe condensation of nuclei after treatment with EDP-M, LEDP-M and L(I)EDP-M (Fig. 12 C-E) compared to controls (Fig. 12B) which was not evident in SJ-ACC3 tumors (Fig. 13 B-E).

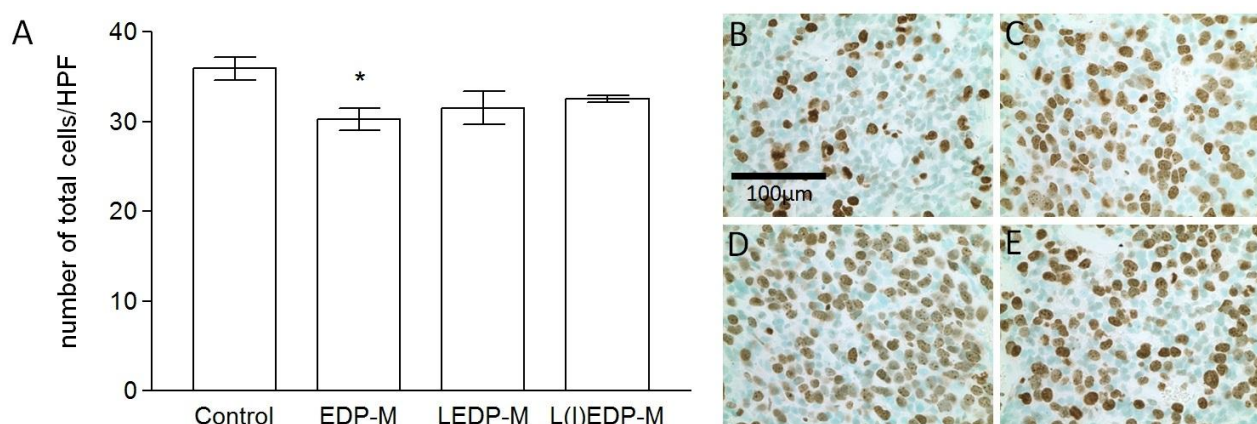


**Fig. 13:** Analysis of SJ-ACC3 tumor tissue obtained from the short-term therapeutic experiment. Using Ki67 immunohistochemistry and methyl green counterstaining, the total number of tumor cells (Ki67-positive and Ki67-negative cells) was quantified (A). Representative pictures for NaCl, EDP-M, LEDP-M and L(I)EDP-M treated tumors are displayed in B-E, respectively. Statistical significance versus controls is denoted with asterisks (\*,  $p < 0.05$ ; \*\*,  $p < 0.01$ ; \*\*\*,  $p < 0.001$ ).

### 3.1.2 Investigation of apoptosis

Tumor tissues of both xenografts models were furthermore investigated utilizing the TUNEL assay to enable a detection of apoptotic cells (protocol see 2.3.4.5). Quantification of apoptosis revealed for both tumor models tendencies towards induction of apoptosis upon the specific therapeutic treatments (SW-13: EDP-M:  $3.0 \pm 0.5$ ,  $p=1.000$ ; LEDP-M  $4.2 \pm 0.7$ ,  $p=0.323$  and L(I)EDP-M  $4.3 \pm 0.9$ ,  $p=0.325$  Fig. 14A; SJ-ACC3: EDP-M:  $5.5 \pm 0.8$ ,  $p=0.280$ ; LEDP-M  $5.1 \pm 0.5$ ,  $p=0.772$  and L(I)EDP-M  $5.4 \pm 0.4$ ,  $p=0.361$  versus controls; Fig. 14B), but the detected values did not reach statistical significance for any treatment in comparison to controls (SW-13:  $2.4 \pm 0.5$ ; SJ-ACC3:  $3.5 \pm 0.8$ ; Fig. 14A and 14B, respectively).

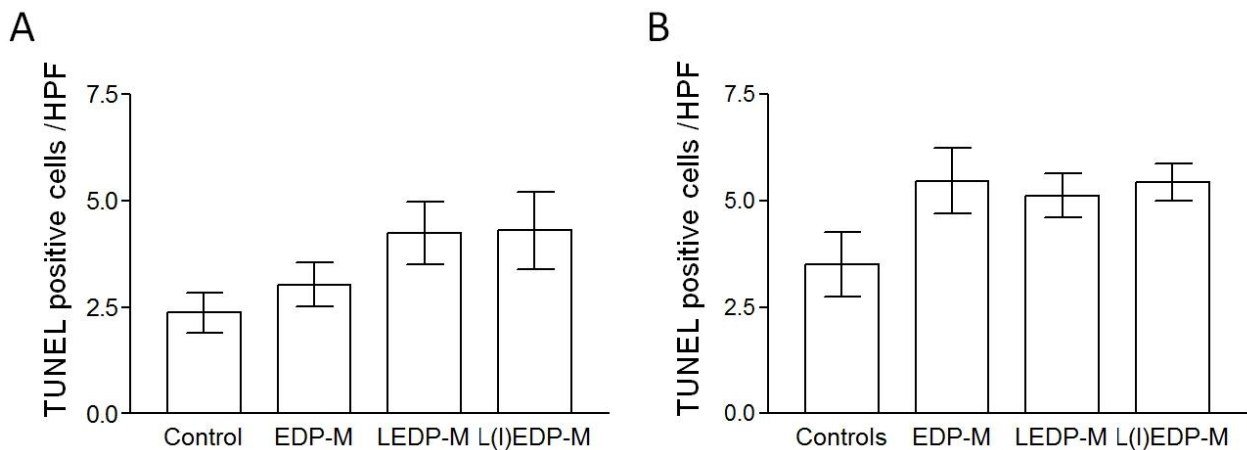


**Fig. 14:** Quantification of TUNEL positive cells in tumor tissue of SW-13 (A) and SJ-ACC3 (B) xenografts. Statistical analysis revealed overall no significant differences in both xenograft models.

### 3.1.3 Histological evaluation of necrosis in tumor tissues

Histological analysis was performed using regressive hematoxylin/eosin staining. For SW-13, the anti-tumoral effects shown for Ki67 immunohistochemistry (see 3.1.1) were thereby histologically confirmed by a semi-quantitative analysis of necrosis using hematoxylin/eosin staining. Each SW-13 tumor was histologically analyzed and categorized regarding necrotic areas (from low to high levels of necrosis with 0 to 3, respectively) as illustrated in Fig. 15M. Representative pictures for these semiquantitative categories are shown in Fig. 15I-L. While

necrosis was rarely detected for the control group, the presence and grades of necrosis increased upon EDP-M over LEDP-M to L(l)-EDP-M administration on SW-13 xenografts as shown in Fig. 15A-D. Such effects were not evident for SJ-ACC3 tumors (Fig. 15E-H).

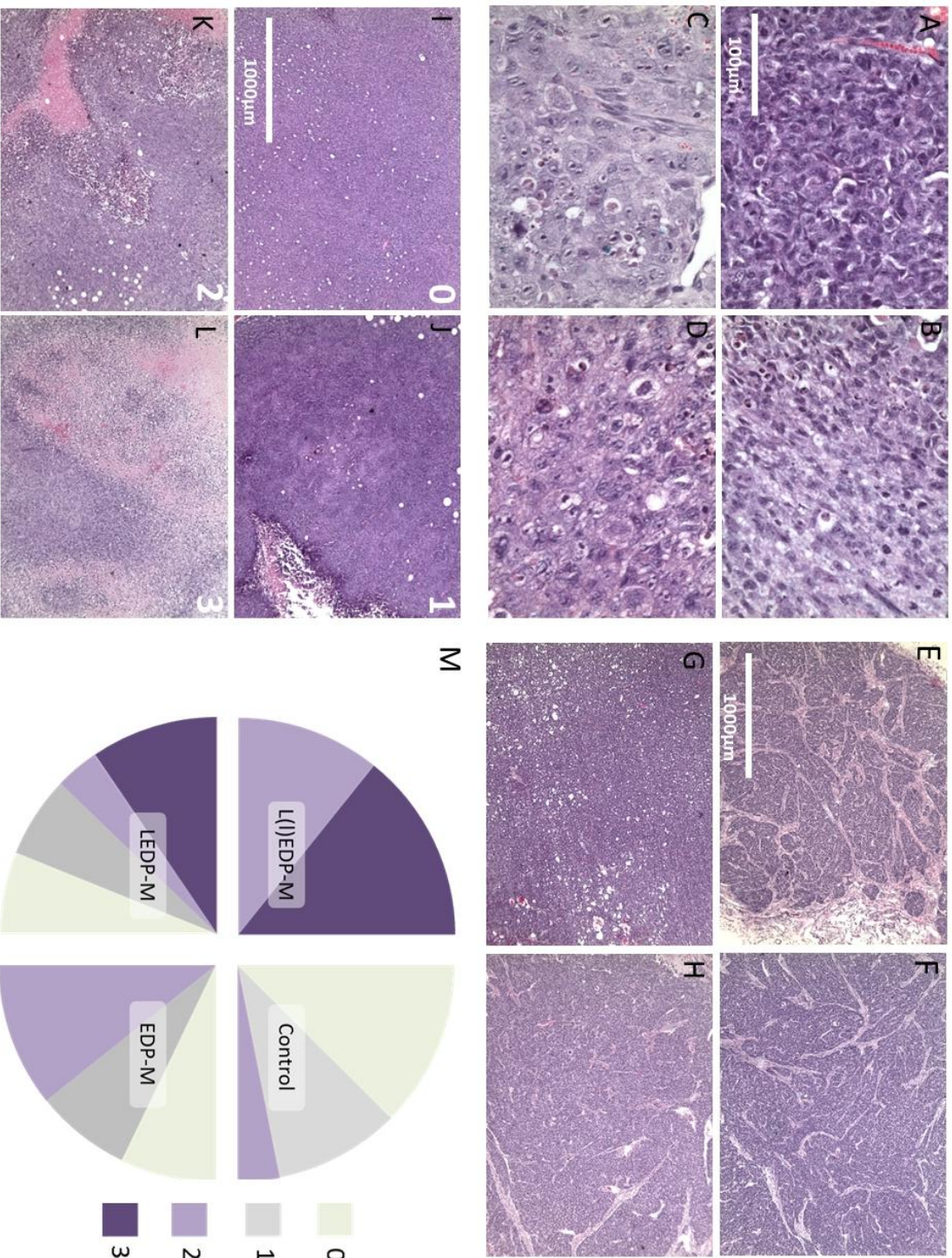


**Fig. 15:** Histological evaluation of SW-13 and SJ-AACC3 tumors derived from short-term experiments after staining with Hematoxylin/Eosin. For SW-13 and SJ-AACC3, representative pictures are shown for NaCl (A, E), EDP-M (B, F), LEDP-M (C, G) and L(I)EDP-M (D, H) treated tumors, respectively. In SW-13 xenografts, necrosis was analyzed with four categories (I-L) ranked in ascending order from 0 (no necrosis) until 3 (extensive necrosis) for each tumor as summarized in (M). An increase of necrotic tissue was not detectable after therapeutic treatment for SJ-AACC3.

### 3.2 Long-term therapeutic efficacy

In subsequent long-term experiments, anti-tumoral effects of the different therapeutic treatments were investigated on SW-13 and SJ-ACC3 tumor bearing mice. Therapeutic regimens and treatment groups were unaltered compared to short-term experiments (see 2.3.3).

In contrast to short-term evaluation, primary endpoint of these long-term studies was the tumor development (expressed as length x width in cm<sup>2</sup>) upon repeated treatment with EDP-M, LEDP-M or L(I)EDP-M (Fig. 16). Between each cycle a therapy free interval of ten days was set.

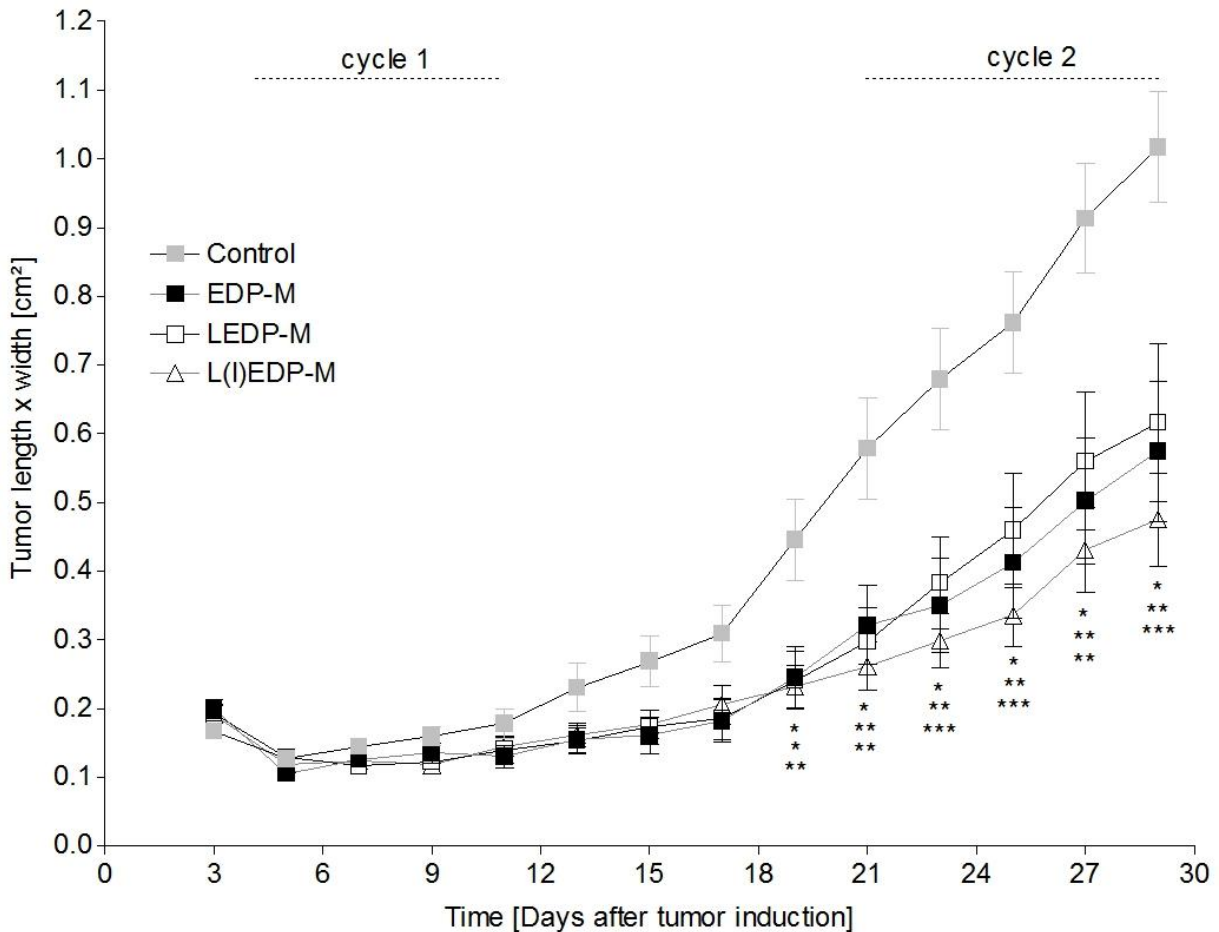


**Fig. 16:** Antitumoral effects of the different treatment protocols on SW-13 xenografts after two therapeutic cycles measured as tumor length x width [cm<sup>2</sup>]. Significant differences compared to controls are illustrated with: \*, p<0.05; \*\*, p<0.01; \*\*\*, p<0.001.

The long-term experiment confirmed the previously obtained results from the SW-13 short-term study and demonstrated anti-tumoral effects for all treatment modalities. Moreover, highest tumor size reduction upon two therapeutic cycles was detected upon L(I)EDP-M treatment compared to controls (cm<sup>2</sup>, day 29 after tumor cell injection, NaCl: 1.02 ± 0.08; EDP-M: 0.57 ± 0.10, p<0.01; LEDP-M 0.62 ± 0.11, p<0.05; L(I)EDP-M: 0.48 ± 0.07, p<0.001, Fig. 16).

In contrast, for SJ-ACC3 no significant differences regarding the tumor development were detectable upon two cycles with the different therapeutic regimens (day 56 post implantation of tumor xenografts, NaCl: 0.30±0.14; EDP-M: 0.14±0.06, p>0.05; LEDP-M 0.12±0.03, p>0.05; L(I)EDP-M: 0.17±0.08, p>0.05; Fig. 17).

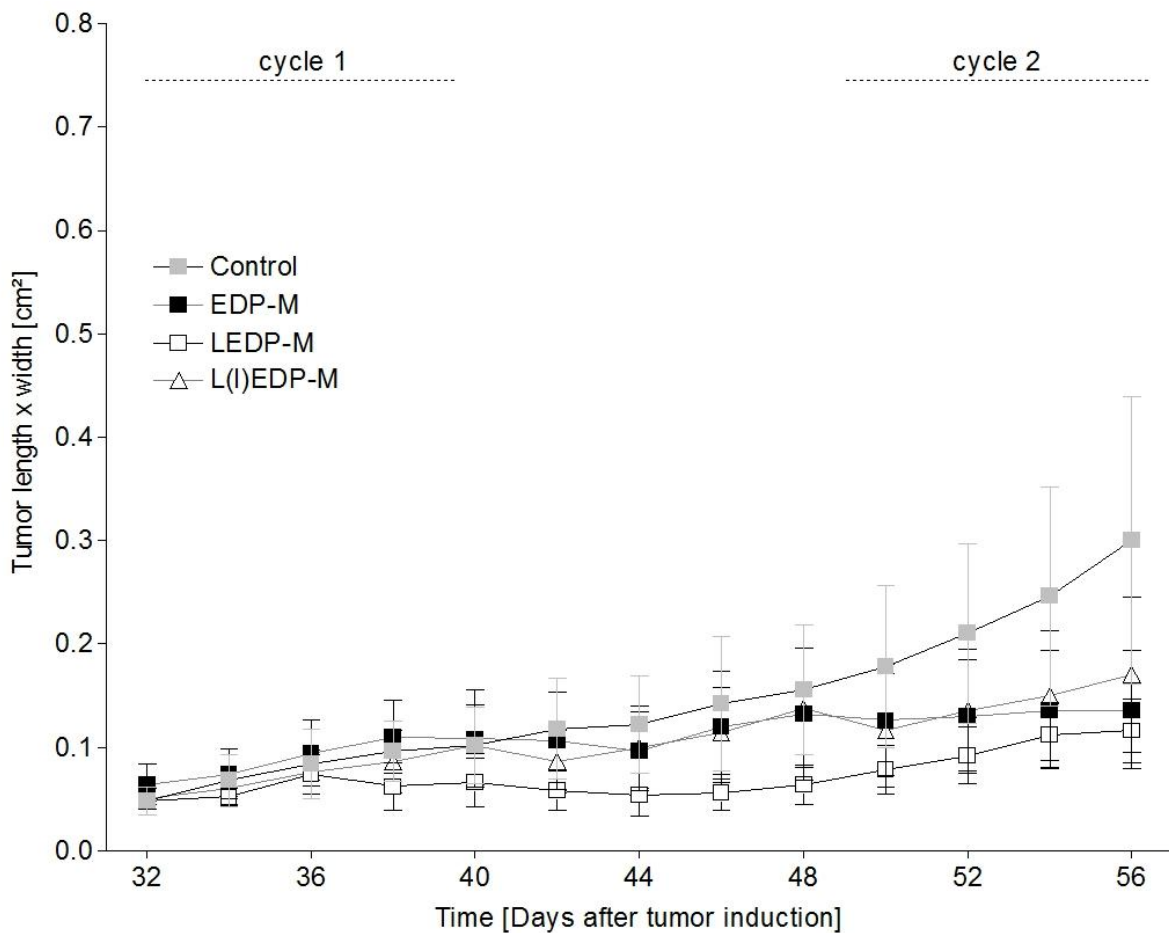


**Fig. 17:** Effects on the SJ-ACC3 tumor xenograft size [cm<sup>2</sup>] after treatment with two therapeutic cycles of the different treatment regimens EDP-M, LEDP-M, L(I)EDP-M and controls.

### 3.3 Tolerability and off-target profiles

To assess the acute tolerability of the different treatment regimens, typical off-target organs of the classical EDP-M regimen were investigated. Moreover, blood samples were analyzed regarding leukocyte count as leukopenia is known to be a well recognized and common dose-limiting side effect of the classical clinical gold standard.

Furthermore, long-term tolerability and overall survival of the different treatment modalities were investigated for up to four treatment cycles.

### 3.4 Analysis of leukocytes upon short-term treatment

Leukocytes count was performed for both xenografts models after one therapeutic treatment cycle and is shown in Fig. 18. The analysis not only confirmed for the classical EDP-M regimen a significant reduced number of leukocytes ( $3.41 \pm 1.37$ ), it also revealed such an effect for the liposomal treatment arms LEDP-M ( $3.81 \pm 1.14$ ) and L(I)EDP-M ( $3.81 \pm 1.30$ ) compared to controls ( $7.19 \pm 2.26$ ,  $p < 0.001$ ).

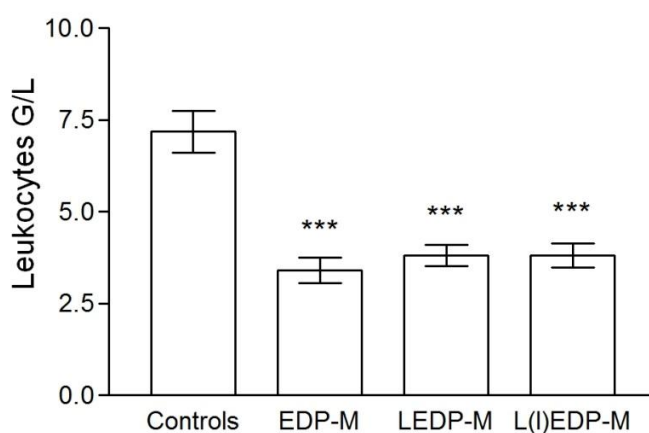


**Fig. 18:** Analysis of leukocyte count after one therapeutic treatment cycle with EDP-M, LEDP-M, L(I)EDP-M and controls in SW-13 and SJ-ACC3 tumor bearing mice. Stars denote significant differences compared with L(I)EDP-M (\*,  $p < 0.05$ ; \*\*,  $p < 0.01$ ; \*\*\*,  $p < 0.001$ ).

### 3.5 Analysis of survival and lethal side-effects upon long-term treatment

In an attempt to investigate the long-term tolerability of the different treatment modalities, therapeutic treatment of SW-13 tumor bearing mice (as already outlined for two cycles in 3.2) was continued for up to four cycles.

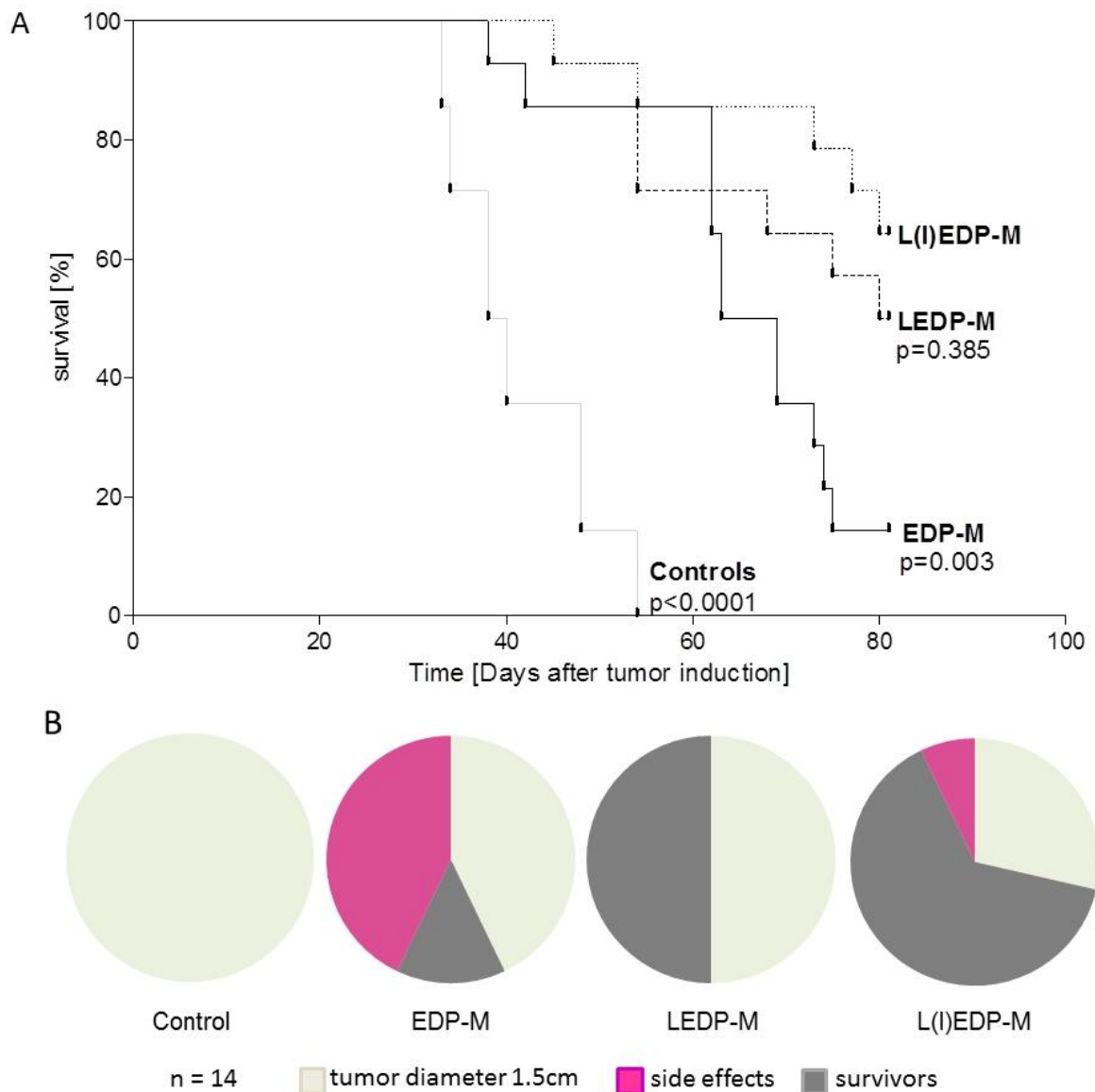


**Fig. 19:** Overall survival (A) and appearance of pre-defined endpoints leading to study determination (B) in the SW-13 long-term study. Treatment of tumor-bearing mice was continued for up to four therapeutic cycles with either NaCl, EDP-M, LEDP-M or L(I)EDP-M. P-values are illustrated for NaCl, EDP-M and LEDP-M compared to L(I)EDP-M treatment (Mantel-Cox (log-rank) analysis).

Following this approach, overall survival was monitored with endpoints such as 1.5 cm longest tumor diameter and appearance of severe adverse effects (such as body weight loss or abnormal body posture) for study determination.

According to these criteria, L(I)EDP-M treatment led to significantly prolonged overall survival not only in comparison to controls ( $p < 0.0001$ ), but also compared to EDP-M ( $p = 0.003$ ) as shown in Fig. 19A. As illustrated in figure 19B, all control animals had to be euthanized due to the longest tumor diameter of 1.5 cm which occurred also in 43% of EDP-M, 50% of LEDP-M and 29% of L(I)EDP-M treated animals. In contrast, treatment with EDP-M led to a pronounced development of side effects (including weight loss and abnormal body posture) in 6 of 14 (43%) cases while LEDP-M (0 of 14, 0%) and L(I)EDP-M (1 of 14, 7%) treatments reduced such incidents (Fig. 19B).

### **3.6 Analysis of hearts and kidneys**

Investigation of kidneys and hearts was also performed after up to four treatment cycles in SW-13 tumor bearing mice as these organs are known to be targeted by classical formulations of cisplatin and doxorubicin.

While HE stainings of kidneys from control mice ( $n = 14$ ) did not reveal any pathological finding, 5 of 14 kidneys in the EDP-M group displayed severe pathologic alterations by occurrence of tubular casts (Fig. 20). Such histological changes were not detectable in the therapeutic arms including liposomal formulations of cisplatin. Specifically, in none of 14 animals treated with LEDP-M and only one of 14 mice treated with L(I)EDP-M minor structural renal alternations were found.

Moreover, also mild cardiotoxic effects were detectable in the EDP-M arm exclusively. While in two of five investigated hearts of the EDP-M group vacuole formation and single cell necrosis could be detected (see Fig. 21), such effects were not apparent in the liposomal treatment groups.

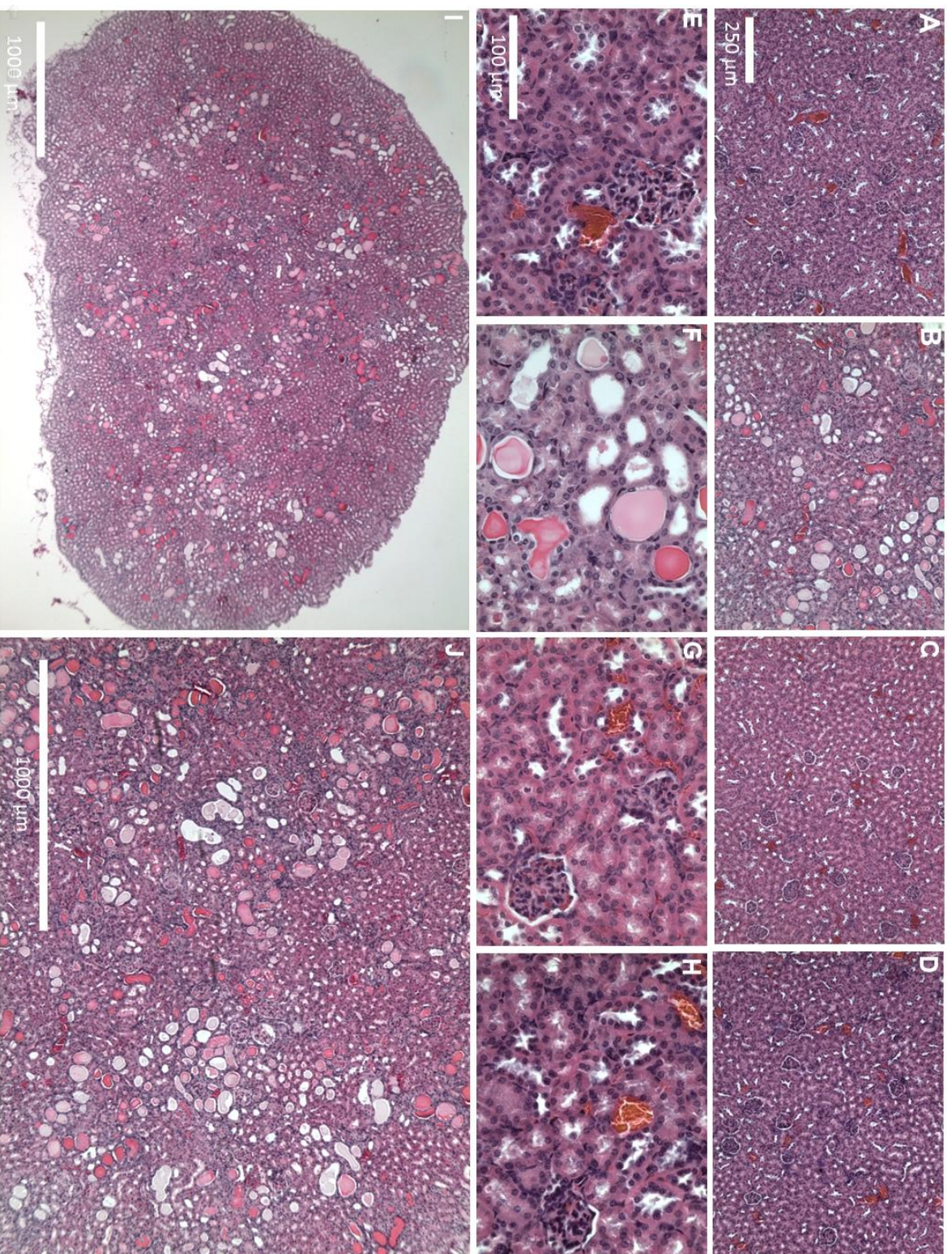


**Fig. 20:** Pathological examination of HE stained kidneys from controls (NaCl) (A, E), EDP-M (B, F), LEDP-M (C, G), L(1)EDP-M (D, H) in 100x (A-D) and 400x (E-H) magnification, respectively. EDP-M treatment led to distinct pathological alteration in kidney tissue, as illustrated in 25x (I) and 500x (J) magnification. Such severe alterations were absent after treatment with LEDP-M and L(1)EDP-M regimens.

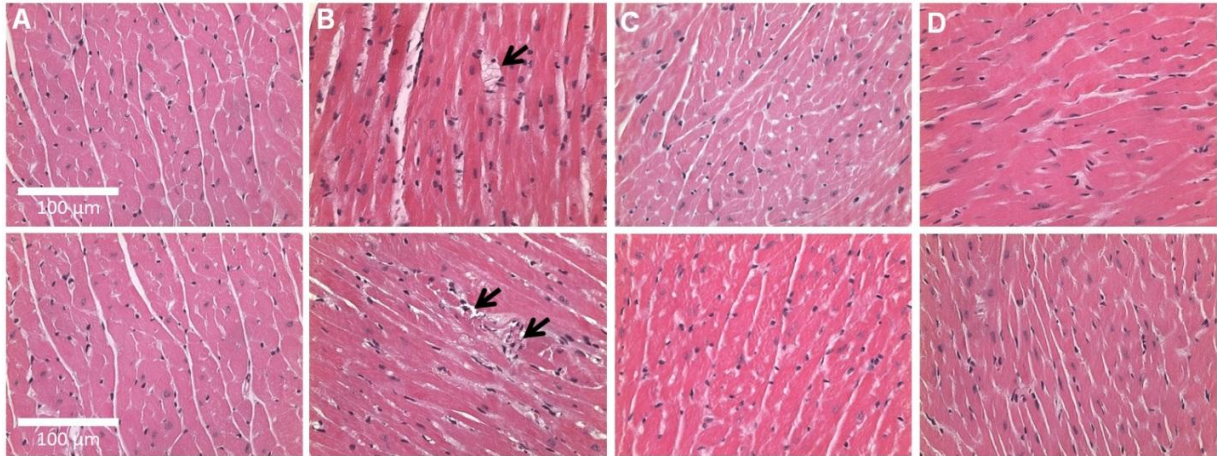


**Fig. 21:** Pathological examination of H&E stained hearts (400x magnification) upon long-term treatment with control (NaCl, A), EDP-M (B), LEDP-M (C) and L(I)EDP-M (D). Black arrows point at vacuole formation and single cell necrosis which occurred exclusively in hearts of mice treated with classical EDP-M regime.

### 3.7 Circulating miR-210 as potential biomarker for therapeutic efficacy

Based on a pilot experiment analyzing a panel of various miRs (miR-195, miR-210, miR-483-3p, miR-483-5p and miR-503) on NaCl, EDP-M and LEDP-M treated NCI-H295R xenografts (data not shown) and data from the literature, two miRs were selected for examination as putative therapeutic biomarkers: miR-483-5p and miR-210. To investigate such a role for the pre-selected miRs, the ratio of intratumoral to circulating miR (miR ratio) was calculated for each individual animal (see chapter 2.4).

After one therapeutic cycle with NaCl or LEDP-M, miR ratio revealed no treatment-dependent changes for miR-483-5p expression in both tumor models (SW-13: control  $1.38 \pm 0.52$ , LEDP-M  $0.81 \pm 0.11$ , SJ-ACC3: control  $1.02 \pm 0.12$ , LEDP-M  $1.74 \pm 0.43$ ; Fig. 22A). In contrast, miR-210 ratio was significantly altered in SW-13 after LEDP-M treatment ( $0.32 \pm 0.06$ ) compared to controls ( $1.20 \pm 0.31$ ) indicating elevated circulating miR-210 levels. Such an effect was not evident for SJ-ACC3 (control  $1.26 \pm 0.74$ , LEDP-M  $0.83 \pm 0.32$ ; Fig. 22B).

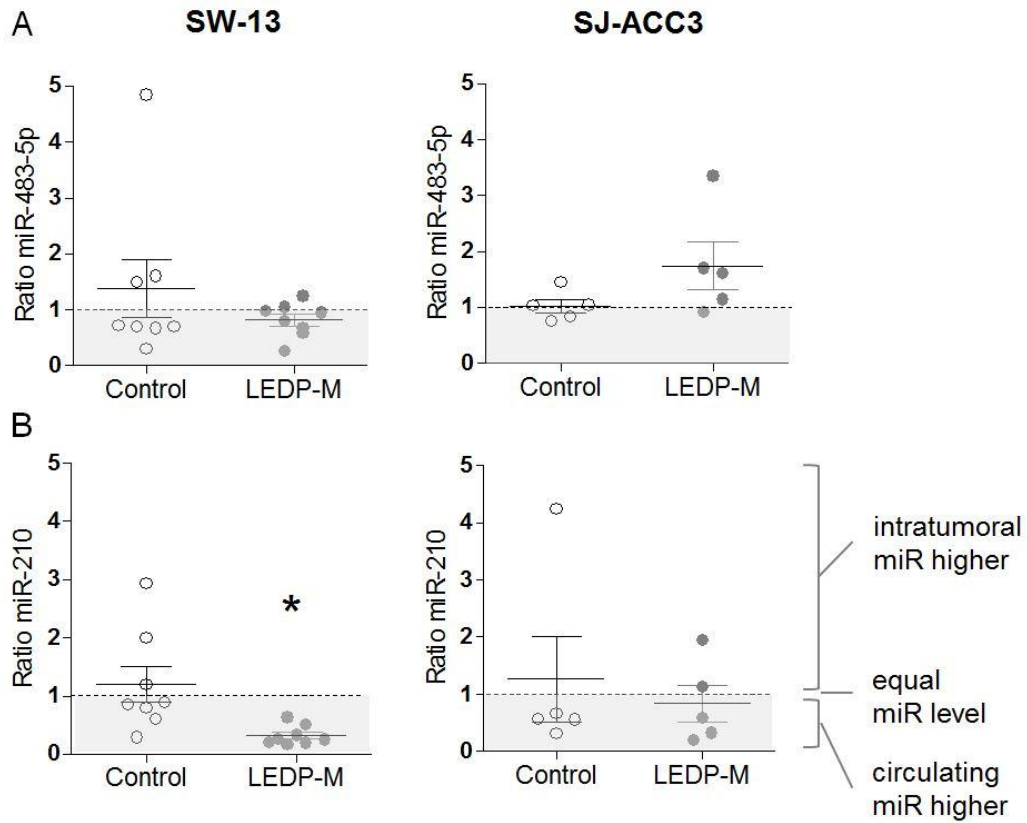


**Fig. 22:** Quantitative Real-Time PCR was performed to analyze intratumoral and circulating microRNA 483-5p (A) and microRNA-210 (B) of control (NaCl) and LEDP-M treated SW-13 and SJ-ACC3 tumor bearing mice. For an evaluation of changes upon antitumoral therapy in each animal, the ratio of intratumoral to circulating miR level was calculated after normalization to controls. A value of 1 suggests equal levels in tumor and plasma sample. A value of  $>1$  indicates an elevated expression of intratumoral microRNA while a ratio of  $<1$  reveals an elevated expression of circulating microRNA. Significant differences are denoted with \*,  $p < 0.05$ .

### **3.8 Clinical data**

Clinical data were obtained within a cooperation project of the university hospitals Wuerzburg and Munich, managed by Prof. Dr. med. Martin Fassnacht-Capeller and Prof. Dr. med. Felix Beuschlein, respectively. For this pilot project, six patients were selected and received a liposomally modified EDP-M scheme (lipEDP-M) including at least one liposomal drug on a compassionate use basis.

In general, the drug regimens were well tolerated. However, none of these heavily pre-treated patients experienced an objective tumor response. Kidney function was clearly impaired in three patients due to earlier EDP-M related renal toxicity. Remarkably, the glomerular filtration rate (measured by MDRD formula) did not further deteriorate during antitumoral therapy with liposomal drug regimens. However, one patient experienced acute kidney failure after receiving the second cycle of lipEDP-M which was most likely due to sepsis. Of particular importance, three of six patients evaluated the liposomally modified regimen better tolerable than the previously administered conventional EDP-M scheme. Two patients mentioned no difference and one study participant experienced no subjective toxicity following EDP-M or lipEDP-M treatment.

patients	liposomal EDP-M (lipEDP-M)											
	EDP-M	reason for liposomal EDP-M	cycles [n]	treatment details	Δ of sum of target lesions	best objective response	serious adverse event	MDRD	individual evaluation of lipEDP-M			
ID	age, sex	cycles [n]	reason for liposomal EDP-M	cycles [n]	treatment details	prior lipEDP-M	post lipEDP-M	best objective response	serious adverse event	prior lipEDP-M	post lipEDP-M	individual evaluation of lipEDP-M
#1	45 y, ♀	12	neuro- and cardio-toxicity	5	c1-2: IP (100 mg/m <sup>2</sup> , d1+2) c3-5: IP (200 mg/m <sup>2</sup> )	n.a.	+30%	PD	-	90	95	no subjective toxicity
#2	47 y, ♀	6 (only EP)	individual wish	3	c1: IP (200 mg/m <sup>2</sup> ) c2-3: IP (200 mg/m <sup>2</sup> ), ID (30 mg/m <sup>2</sup> )	+40%	n.a. <sup>c</sup>	PD	seizure, oculo-motor nerve palsy <sup>d</sup>	88	87	better tolerated
#3	65 y, ♀	6	renal function	1	adjuvantly ED+ IP (200 mg/m <sup>2</sup> )	radical surgery	new lesions	PD	-	37	49	less toxic
#4	65 y, ♂	3	renal function	2	ED + IP (100 mg/m <sup>2</sup> , d3+4)	-10%	+75%	PD	sepsis, acute kidney failure	36	32	better tolerated
#5	43 y, ♂	8	individual wish	2	E + ID (40 mg/m <sup>2</sup> ) + P	+25%	+25%	PD	-	68	65	no difference
#6	55 y, ♂	14 <sup>a</sup>	- <sup>b</sup>	2	E + ID (30 mg/m <sup>2</sup> ), carboplatin AUC 4	+26%	+21%	PD	thrombocytopenia and anemia, both CTC 3	48	49	no difference

<sup>a</sup> P was replaced by carboplatin, <sup>b</sup> no specific toxicity, but PD and high cumulative dosage of doxorubicin, <sup>c</sup> due to palliative situation (increasing cerebral metastases) no formal tumor evaluation was performed, <sup>d</sup> most likely due to newly diagnosed carcinomatous meningitis

C: cycle, D: doxorubicin, E: etoposide, ID: liposomal doxorubicin (myocet™), IP: liposomal cisplatin (lipoplatin™), MDRD formula: ml/min/1,73 m<sup>2</sup>, n: number, n.a.: not available, P: cisplatin, PD: progressive disease, y: years, ♂: male, ♀: female, Δ: change

**Tab. 10:** Illustration of first clinical data for the investigation of liposomally modified EDP-M (lipEDP-M) in six patients with very advanced ACC. Patient recruitment, data collection and evaluation was performed in a cooperation project of Wuerzburg and Munich.

#### **4. Discussion**

Clinical translation of novel therapeutic regimens for adrenocortical carcinoma (ACC) remains challenging, particularly due to observed tumor heterogeneity regarding tumor growth rate, treatment response and overall survival. Furthermore, ACC exhibit different subtypes as for example adult vs. pediatric and hormonally active vs. hormonal inactive tumors. Combination chemotherapy including etoposide, doxorubicin and cisplatin together with mitotane (EDP-M) represents the current systemic standard protocol for advanced ACC, which are not amenable for surgery [9]. Despite surgical and therapeutic intervention, ACC are conflicted by a very poor prognosis and unfavorable long-term survival outcome [3]. Classical therapeutic treatment with multi-chemotherapeutic regimens as EDP-M induces severe and dose-limiting adverse effects [1, 9, 10]. Moreover, high variability in therapeutic responsiveness [55] makes it almost impossible for physicians to weigh patients' long-term benefit and life quality against highly toxic combination chemotherapy protocols. Therefore, the most pivotal tasks to be accomplished are the development of more effective, but also more tolerable therapeutic regimens. Another important aim is the establishment of reliable therapeutic biomarkers which help to distinguish reasonable therapeutic consequences for ACC patients [56].

#### 4.1 Therapeutic efficacy of liposomal EDP-M regimens

In the present study, antitumoral efficacies of the classical EDP-M regimen as well as of two novel liposomal protocols (LEDP-M and L(I)EDP-M) were evaluated after short-term and long-term treatment in two different tumor xenograft models for ACC (SW-13 and SJ-ACC3).

For SW-13, both classical and liposomal treatment regimens led to antitumoral effects after one therapeutic cycle revealing the highest efficacy in the liposomal arms regarding tumor cell proliferation and induction of necrosis. In particular, L(I)EDP-M led to a highly significant reduction in tumor cell count, accompanied by a distinct induction of necrosis following one therapeutic cycle. Subsequent long-term experiments confirmed these findings and demonstrated a significant reduction of tumor size in all treatment arms accompanied by improved overall survival with LEDP-M and L(I)EDP-M treatment.

In general, a higher antitumoral efficacy of liposomal regimens can be explained by the occurrence of passive tumor targeting and prolonged plasma stability as reported for liposomal carriers [14, 22]. Moreover, the observed antitumoral efficacy of both liposomal regimens is in accordance with existing preclinical data for ACC. Hantel et al. demonstrated that the tumor cell lines NCI-H295 and SW-13 are characterized by an extraordinary uptake phenomenon of liposomes which supports the application of liposomal drugs for this tumor entity [27]. Accordingly, a recent *in vivo* study using NCI-H295 xenografts demonstrated that LEDP-M treatment led to a significant reduction of tumor sizes compared with the classical scheme composed of EDP-M [28]. Thus, the present study utilizing SW-13 xenografts supports the previous experiments on NCI-H295R xenografts [28] and predicts superior therapeutic efficacies of liposomal treatments chemotherapies for adult ACC. Liposomal chemotherapies have successfully been applied in clinical practice for a wide range of tumor entities [17, 57-59] and therefore represent a therapeutic tool which could be rapidly transferred into clinical use.

In contrast to the effects obtained for NCI-H295R and SW-13, liposomal treatment regimens were not effective against SJ-ACC3, a tumor model of pediatric origin. For this xenograft model slight therapeutic responsiveness was observed upon one therapeutic cycle with classical EDP-M, exclusively. Regarding long-term efficacy, none of the investigated treatment schemes induced a significant therapeutic response.

These findings are consistent with the fact that pediatric ACC patients demonstrate even with surgical and chemotherapeutic intervention a very poor prognosis and low tumor response [60].

ACC occurring in early childhood represent a distinct entity compared to adult ACCs with regards to their origin, clinical manifestation, molecular profiles and prognosis [61]. Together with their low prevalence, this aggravates the situation to find effective treatment options for these tumors [61, 62]. Also, acute and long-term complications of highly toxic regimens as EDP-M are of crucial importance in the therapy of children and deserve special attention as current medical treatment options lead to irreversible off-target effects and impairments [9, 60].

In both pediatric and adult ACC, the most commonly used combination for ACC treatment is EDP in combination with mitotane [9, 10, 60, 63]. In adult patients, mitotane is the only approved drug for ACC treatment but for pediatric ACC the use of mitotane has not been evaluated systematically [64]. Only recently, a preclinical study of Pinto et al. [38] demonstrated that single-agent therapy with cisplatin, but not with etoposide and doxorubicin, induced potent anti-tumoral effects. In addition, the study identified topotecan as a potentially effective agent for the treatment of pediatric ACC. Liposomal cisplatin (lipoplatin™) is already under clinical investigation (phase I, II and III trials) and also liposomal topotecan is preclinically evaluated for other tumor entities [13, 23-25, 57, 65, 66]. Accordingly, a combinatorial approach of liposomal formulations of cisplatin and topotecan could represent an interesting strategy to improve therapeutic benefit and tolerability for pediatric ACC patients in the future.

## 4.2 Off-target profiles of liposomal EDP-M regimens in preclinical tumor xenografts

Regarding the clinical application of EDP-M protocols, not only therapeutic benefit but also tolerability including acute and long-term complications have main impact on clinical applicability [1, 56]. The combination chemotherapy protocol including the cytotoxic drugs etoposide, doxorubicin and cisplatin induces highly toxic off-target effects characterized by dose-limiting hematological toxicities, gastrointestinal impairment and other toxicities as irreversible cardiotoxic and nephrotoxic events [9, 10].

As one example, dose-limiting leucopenia is a known and common complication [9]. Unfavorably and confirming the results of Hantel et al. 2014 [28], leukocyte counts were reduced not only after treatment with EDP-M and LEDP-M, but also in the L(I)EDP-M regimen in this recent study. Interestingly, even though other *in vivo* studies demonstrated for liposomal etoposide higher maximal tolerable doses, the same experiments revealed still an induction of myelosuppression [67, 68]. Thus, overall an improvement of clinically observed leucopenia is not to be expected in the administration of liposomal EDP-M regimens.

In addition, also nephrotoxicity and cardiotoxicity impede the application of EDP-M in clinics. Nephrotoxicity is the main dose-limiting side effect of cisplatin therapy. The most serious and common presentation is acute kidney injury which occurs in 20-30% of cisplatin-treated patients [69]. Also, following doxorubicin treatment, approximately one out of four patients experiences congestive heart failure after exceeding cumulative doses of 500 mg/m<sup>2</sup> [11, 70]. More recent data furthermore indicate development of cardiomyopathy after anthracycline-based chemotherapy not only at much lower cumulative doses but even after 4 to 20 years in almost 25% of patients [12, 71]. These findings are of decisive importance not only for adult patients, but also especially for children, given that cytotoxic effects of anthracyclines are generally thought to be irreversible [11]. Such impairments have been studied and described extensively in the literature and are known to be common adverse effects of doxorubicin and cisplatin, respectively [11, 57, 69, 72, 73].

In the present study, kidneys and hearts were histologically assessed following multiple treatment cycles with EDP-M. Histological evaluation confirmed pathological alterations upon EDP-M therapy in kidneys and hearts compared to controls revealing massive tubular casts and a development of myocyte necrosis and vacuole formation, respectively. LEDP-M and L(I)EDP-M protocols were very likely to improve off-target profiles as liposomal doxorubicin and liposomal cisplatin have both been extensively studied in this context [17, 25, 57, 74-76]. In recent years,

several clinical studies have provided evidence for a highly significant reduction of cardiotoxicity [14, 74] and nephrotoxicity [13, 57, 76] using liposomal formulations of doxorubicin and cisplatin instead of their parental drugs.

In the current study, the analysis of kidneys and hearts upon liposomal treatment clearly confirmed an improvement of such off-target profiles in comparison to classical EDP-M treatment. Even after up to four treatment cycles no comparable cardiotoxic and nephrotoxic impairment was detectable upon treatment with LEDP-M or L(I)EDP-M.

In addition, overall survival upon multiple treatment cycles was analyzed including not only a monitoring of the longest tumor diameter, but also a surveillance of adverse effects using pre-defined criteria for study determination. While a high number of EDP-M treated animals developed side-effects as body weight loss and abnormal body posture, comparable effects were not apparent upon treatment with liposomal regimens. Therefore, the present study furthermore demonstrates significantly increased tolerability of L(I)EDP-M treatment compared to EDP-M regimen.

### 4.3 MiR-483-5p and miR-210 as therapeutic biomarkers for ACC

Despite an improvement of therapeutic efficacy and off-target profiles, quality of life during and after therapeutic treatment with highly toxic regimen is of pivotal interest for patients in clinical practice. ACC are characterized by high heterogeneity mostly with highly malignant and progressive potential. However, in rare cases ACC can also reveal a more indolent and less aggressive phenotype [9, 10]. Accordingly, the therapeutic responsiveness upon EDP-M can range from high to completely ineffective. Rarely observed long-term cures combined with irreversible side-effects of EDP-M treatment furthermore worsen the situation for physicians and treated ACC patients. As appropriate markers for therapeutic efficacy do not exist [56], the assessment and weighing of multiple EDP-M treatment cycles against long-term benefit and quality of life remains an almost untraceable task in clinical practice.

In recent years, increased attention has been drawn to the analysis and quantification of micro-RNA (miR). MiR are defined as small non-coding RNA molecules and are influencing the gene expression, thereby representing important regulators for physiological and pathological conditions as well as tumorigenesis [40, 43]. For a variety of tumor entities including ACC, specific signatures of aberrant miR expression patterns have been demonstrated [40, 43]. Progression of cancer, therapeutic response and survival rates have been correlated with levels of circulating miRs in several studies. Such investigations of blood samples indicate the potential of miR to monitor therapeutic responses applying minimal invasive techniques [8, 40].

In this research project, miR-483-5p and miR-210 levels in tumors and plasma exosomes were investigated as potentially interesting therapeutic biomarkers for ACC. The *MIR483* gene is located in the second intron of the *IGF2* gene and high miR-483-5p was found to be paralleled by high expression of *IGF2* and to correlate with malignancy in ACC [43, 45]. For miR-210, also known as hypoxia-inducible miR-210 or “micromanager of the hypoxia pathway” [50], an involvement in cell cycle regulation, mitochondrial metabolism, DNA repair mechanisms and angiogenesis has been reported [50, 51]. Regarding ACC, high miR-210 levels have been correlated with parameters of tumor aggressiveness as well as clinical outcome [44]. Similar findings have been reported for a variety of other tumor entities in clinical studies [46-48, 77].

SW-13 and SJ-ACC3 tumor tissue and plasma exosomes were analyzed after one therapeutic cycle with control (NaCl) or LEDP-M treatment, as LEDP-M had revealed anti-tumoral efficacy in SW-13 but not in SJ-ACC3. For each animal, the ratio of intratumoral to circulating miR was

calculated to detect individual treatment-dependent changes in tumor and circulating miR. In this setting, investigation of miR-483-5p revealed no treatment-related changes. However, for SW-13 significantly altered miR-210 ratio could be detected, which resulted from elevated circulating miR-210 levels following LEDP-M treatment.

This finding is in accordance with a clinical study investigating miR-210 level following neoadjuvant therapy in breast cancer patients. In this present study, increased miR-210 levels after therapy could be detected. However, in this study this finding could not be correlated with a long-term outcome so far [78]. Thus, as SW-13, but not SJ-ACC3, responded to LEDP-M therapy and significant alterations in circulating mir-210 ratio were detected exclusively for SW-13 upon treatment, miR-210 could represent a potentially interesting therapeutic biomarker for ACC.

However, additional investigations are required to further clarify the underlying mechanisms of altered circulating miR levels. One important factor could be the influence of the individual therapy (as classical or liposomal chemotherapy) on miR levels [43]. Liposomes might interfere with the formation of exosomes which could affect the analysis and the following results. Furthermore, a correlation of therapeutic response and changes in miR ratio needs to be studied at different time points following therapeutic intervention as time-dependent fluctuations in miR level upon therapy are not clarified yet in detail [79]. Studies which investigated miR levels after different therapeutic interventions include a monitoring of miR levels from two weeks up to six months post treatment [79-81]. In the present study, animals were sacrificed 48 hours after the final treatment and therefore this recent miR analysis includes only one time point. Additional investigations considering these factors would be of high importance in order to establish miR-210 as a therapeutic biomarker. Such a biomarker would be helpful assessing treatment efficacy and thereby improving the situation for ACC patients.

#### 4.4 Liposomally modified EDP-M in clinics

Approaches to the development of novel therapeutic biomarkers for ACC treatment should be seen in the context of long-term projects for the future. This perception stands in contrast to the administration of liposomal doxorubicin and cisplatin for ACC patients as such formulations are already administered for a variety of other malignancies [14, 19, 22, 57]. As caelyx™ and lipoplatin™ are already in clinical use for other tumor entities [13, 22], efficient transfer of LEDP-M into clinical practice would be possible and could be rapidly achieved.

After promising results of the described preclinical experiments and in view of potential benefits for patients, liposomally modified EDP-M protocols were investigated in six patients revealing advanced ACC tumors. This pilot project of the two ACC centers in Wuerzburg and Munich was supervised by Prof. Dr. med. Martin Fassnacht-Capeller and Prof. Dr. med. Felix Beuschlein, respectively. The investigation of this small patient cohort treated with liposomally modified EDP-M regimen demonstrated for the first time that liposomal chemotherapies in ACC patients were overall well tolerated. Even though antitumoral effects could not be observed in these patients, it should be taken into consideration that all enrolled patients were heavily pre-treated including standard EDP-M and other cytotoxic drugs. Consequently, the observation that none of the patients experienced an objective tumor response has to be seen in the context of very advanced disease [82] and pre-treatment with standard EDP-M, which makes induction of drug resistance more likely [83]. Therefore, this setting might not represent the optimal time point for a therapeutic intervention with liposomal preparations.

In conclusion, an implementation of liposomal cisplatin (lipoplatin™) and doxorubicin (caelyx™, myocet™) would allow a swift clinical translation, could increase therapeutic efficacy, but mainly improve tolerability and thereby quality of life for ACC patients with advanced disease.

## 4.5 Perspectives and outlook

High antitumoral efficacy of liposomal preparations and high dose-limiting toxicity of existing multi-chemotherapeutic regimen have led to the idea to adapt and re-establish clinical treatment schemes for ACC. The fact that recent preliminary data demonstrate successful application of liposomal drugs in ACC patients might represent the starting point to reconsider, modify and change existing treatment protocols of ACC in general.

Liposomally modified EDP-M protocols including liposomal formulations of cisplatin (lipoplatin™) and/or doxorubicin (myocet™, caelyx™) hold great potential to improve the current medical situation in the treatment of ACC. Furthermore, the promising results of this preclinical study including the first successful application of liposomally modified EDP-M in patients recently initiated an EMA (European Medical Agency) orphan drug status application for lipoplatin™ in ACC treatment. Accordingly, most recent plans for a design of novel clinical trials include lipoplatin™ in a larger patient cohort. The idea to use single agent cisplatin therapy with or without mitotane transpired already years ago, but was mainly limited by occurring toxicities [84, 85]. Due to its improved tolerability, lipoplatin™ could be used in higher doses as conventional cisplatin and could also be combined with low-radiation therapy or mitotane in adjuvant therapeutic settings after radical resection or advanced disease patients [84, 86].

Thus, the described findings demonstrate the potential to have a great impact on clinical ACC treatments and could thereby improve therapeutic outcome and life quality of ACC patients in the near future.

## 5. Summary

Adrenocortical carcinoma (ACC) is a rare but highly heterogeneous malignancy. Severe dose-limiting adverse effects and heterogeneous tumor response strictly limit systemic therapy of ACC. Most recent preclinical investigations revealed for LEDP-M (etoposide, liposomal doxorubicin, liposomal cisplatin, mitotane), a liposomal variant of the classical clinical gold-standard EDP-M (etoposide, doxorubicin, cisplatin, mitotane), enhanced anti-tumoral activity. To further increase therapeutic efficacy and improve off-target profiles, this study aimed at the investigation of novel liposomal EDP-M regimens in additional preclinical experiments. For this purpose, hormonally inactive SW-13 and pediatric SJ-ACC xenografts were utilized. In addition to EDP-M and LEDP-M, also a novel therapeutic regimen L(I)EDP-M including liposomal etoposide (liposomal etoposide, liposomal doxorubicin, liposomal cisplatin, mitotane) was investigated and assessed. Preclinical experiments were performed in short-term and long-term settings to investigate anti-tumoral efficacy and side-effects of the different treatment protocols. Moreover, the potential of plasma microRNA-210 to be utilized as a therapeutic biomarker was evaluated. The novel liposomal regimen demonstrated highest anti-proliferative efficacy against SW-13 xenografts, while in SJ-ACC3 tumors only EDP-M was slightly effective. Moreover, overall survival was improved in SW-13 tumor bearing mice after treatment with L(I)EDP-M compared with controls ( $p < 0.0001$ ) and EDP-M ( $p = 0.003$ ). Elevated circulating microRNA-210 levels were evident for the LEDP-M responsive SW-13 tumor model, but not for therapy resistant SJ-ACC xenografts. Consequently, circulating microRNA-210 could be demonstrated to serve as potential biomarker for therapeutic response. Of particular importance for clinical application, histological evaluation of hearts and kidneys demonstrated improved toxicity profiles upon treatment with liposomal regimens. Following these promising results, a small number of ACC patients was treated with a liposomal chemotherapy protocol. Confirming the preclinical results, initial clinical data indicate an improved tolerability of liposomal modified EDP-M. In conclusion, liposomally modified EDP-M regimens represent promising treatment options which bear the potential to improve clinical treatment of ACC in the near future.

## Zusammenfassung

Nebennierenrindenzarzinome (NN-Ca) sind sehr seltene und hochmaligne Tumore. Die Effektivität systemischer Therapieansätze ist für diese sehr heterogene und aggressive Tumorentität oft unbefriedigend und mit starken, dosis-limitierenden Nebenwirkungen verbunden. Neue präklinische Ergebnisse zeigen, dass im Vergleich zum klassischen klinischen Goldstandard EDP-M (Etoposid, Doxorubicin, Cisplatin, Mitotane) ein liposomal modifiziertes Protokoll LEDP-M (Etoposid, liposomales Doxorubicin, liposomales Cisplatin, Mitotane) stärkere antitumorale Effekte zeigt. Ziel dieses Projektes war es, die therapeutische Wirksamkeit sowie die Nebenwirkungsprofile neuer liposomaler Therapieregime in weiteren präklinischen Studien zu untersuchen. Hierfür wurden hormonell inaktive SW-13 Zellen und das pädiatrische SJ-ACC3 Tumormodell als Xenograftmodelle verwendet. Neben klassischer EDP-M und LEDP-M Behandlung wurde ein weiteres liposomales Therapieschema L(I)EDP-M mit liposomalem Etoposid untersucht. Die präklinischen Experimente erfolgten in Kurzzeit- und Langzeitversuchen, in denen antitumorale Wirksamkeit und das Nebenwirkungsspektrum untersucht wurden. Die liposomalen Behandlungsprotokolle zeigten die höchste antitumorale Wirksamkeit im SW-13 Tumormodell, während SJ-ACC3 nur schwach auf die klassische EDP-M Behandlung ansprach. Zudem erbrachte die Analyse der Überlebensrate im SW-13 Modell eine signifikante Verbesserung des Gesamtüberlebens nach L(I)EDP-M Behandlung im Vergleich zu Kontrollen ( $p < 0.0001$ ) und klassischem EDP-M Protokoll ( $p = 0.003$ ). Darüber hinaus wurde zirkulierende microRNA-210 als potentieller therapeutischer Biomarker für NNR-Ca untersucht. Hierbei konnte für zirkulierende microRNA-210 ein Potential als therapeutischer Biomarker nachgewiesen werden, welche exklusiv im therapiesensitiven SW-13 Modell nach LEDP-M Behandlung signifikant erhöht ( $p < 0.05$ ) war. Die histologische Analyse von Herzen und Nieren ergab für die liposomalen Behandlungsprotokolle ein verbessertes Nebenwirkungsprofil verglichen mit dem klassischen EDP-M Therapieregime. Erste klinische Daten stützen diese Ergebnisse mit einer besseren Verträglichkeit eines liposomalen EDP-M Behandlungsregimes. Zusammenfassend stellt ein liposomal modifiziertes EDP-M Behandlungsschema damit eine vielversprechende Behandlungsoption für Patienten mit NNR-Ca dar. Ein liposomales EDP-M Regime könnte bereits in naher Zukunft in klinische Studien überführt werden und würde die Therapie von NNR-Ca vor allem im Bezug auf Verträglichkeit und Behandlungswirksamkeit verbessern.

## 6. References

1. Fassnacht, M., M. Kroiss, and B. Allolio, *Update in adrenocortical carcinoma*. J Clin Endocrinol Metab, 2013. **98**(12): p. 4551-64.
2. Libe, R., et al., *Prognostic factors in stage III-IV adrenocortical carcinomas (ACC): an European Network for the Study of Adrenal Tumor (ENSAT) study*. Ann Oncol, 2015. **26**(10): p. 2119-25.
3. Allolio, B. and M. Fassnacht, *Clinical review: Adrenocortical carcinoma: clinical update*. J Clin Endocrinol Metab, 2006. **91**(6): p. 2027-37.
4. Lebastchi, A.H., J.W. Kunstman, and T. Carling, *Adrenocortical Carcinoma: Current Therapeutic State-of-the-Art*. J Oncol, 2012. **2012**: p. 234726.
5. Else, T., et al., *Adrenocortical carcinoma*. Endocr Rev, 2014. **35**(2): p. 282-326.
6. Pommier, R.F. and M.F. Brennan, *An eleven-year experience with adrenocortical carcinoma*. Surgery, 1992. **112**(6): p. 963-70; discussion 970-1.
7. Terzolo, M., et al., *Adjuvant mitotane treatment for adrenocortical carcinoma*. N Engl J Med, 2007. **356**(23): p. 2372-80.
8. Allolio, B., et al., *Management of adrenocortical carcinoma*. Clin Endocrinol (Oxf), 2004. **60**(3): p. 273-87.
9. Fassnacht, M., et al., *Combination chemotherapy in advanced adrenocortical carcinoma*. N Engl J Med, 2012. **366**(23): p. 2189-97.
10. Berruti, A., et al., *Etoposide, doxorubicin and cisplatin plus mitotane in the treatment of advanced adrenocortical carcinoma: a large prospective phase II trial*. Endocr Relat Cancer, 2005. **12**(3): p. 657-66.
11. Rahman, A.M., S.W. Yusuf, and M.S. Ewer, *Anthracycline-induced cardiotoxicity and the cardiac-sparing effect of liposomal formulation*. Int J Nanomedicine, 2007. **2**(4): p. 567-83.
12. Hequet, O., et al., *Subclinical late cardiomyopathy after doxorubicin therapy for lymphoma in adults*. J Clin Oncol, 2004. **22**(10): p. 1864-71.
13. Boulikas, T., *Clinical overview on Lipoplatin: a successful liposomal formulation of cisplatin*. Expert Opin Investig Drugs, 2009. **18**(8): p. 1197-218.

14. Gabizon, A., H. Shmeeda, and T. Grenader, *Pharmacological basis of pegylated liposomal doxorubicin: impact on cancer therapy*. Eur J Pharm Sci, 2012. **45**(4): p. 388-98.
15. Drummond, D.C., et al., *Optimizing liposomes for delivery of chemotherapeutic agents to solid tumors*. Pharmacol Rev, 1999. **51**(4): p. 691-743.
16. Huwyler, J., J. Drewe, and S. Krahenbuhl, *Tumor targeting using liposomal antineoplastic drugs*. Int J Nanomedicine, 2008. **3**(1): p. 21-9.
17. Gabizon, A., H. Shmeeda, and Y. Barenholz, *Pharmacokinetics of pegylated liposomal Doxorubicin: review of animal and human studies*. Clin Pharmacokinet, 2003. **42**(5): p. 419-36.
18. Immordino, M.L., F. Dosio, and L. Cattel, *Stealth liposomes: review of the basic science, rationale, and clinical applications, existing and potential*. Int J Nanomedicine, 2006. **1**(3): p. 297-315.
19. Bozzuto, G. and A. Molinari, *Liposomes as nanomedical devices*. Int J Nanomedicine, 2015. **10**: p. 975-99.
20. Duncan, R., *The dawning era of polymer therapeutics*. Nat Rev Drug Discov, 2003. **2**(5): p. 347-60.
21. Maeda, H., et al., *Tumor vascular permeability and the EPR effect in macromolecular therapeutics: a review*. J Control Release, 2000. **65**(1-2): p. 271-84.
22. Marchal, S., et al., *Anticancer Drug Delivery: An Update on Clinically Applied Nanotherapeutics*. Drugs, 2015. **75**(14): p. 1601-11.
23. Stathopoulos, G.P., et al., *Comparison of liposomal cisplatin versus cisplatin in non-squamous cell non-small-cell lung cancer*. Cancer Chemother Pharmacol, 2011. **68**(4): p. 945-50.
24. Stathopoulos, G.P., et al., *Liposomal cisplatin combined with gemcitabine in pretreated advanced pancreatic cancer patients: a phase I-II study*. Oncol Rep, 2006. **15**(5): p. 1201-4.
25. Mylonakis, N., et al., *Phase II study of liposomal cisplatin (Lipoplatin) plus gemcitabine versus cisplatin plus gemcitabine as first line treatment in inoperable (stage IIIB/IV) non-small cell lung cancer*. Lung Cancer, 2010. **68**(2): p. 240-7.
26. Najar, I.A. and R.K. Johri, *Pharmaceutical and pharmacological approaches for bioavailability enhancement of etoposide*. J Biosci, 2014. **39**(1): p. 139-44.
27. Hantel, C., et al., *Liposomal doxorubicin-based treatment in a preclinical model of adrenocortical carcinoma*. J Endocrinol, 2012. **213**(2): p. 155-61.

28. Hantel, C., et al., *Liposomal polychemotherapy improves adrenocortical carcinoma treatment in a preclinical rodent model*. *Endocr Relat Cancer*, 2014. **21**(3): p. 383-94.
29. Hantel, C., et al., *Anti insulin-like growth factor I receptor immunoliposomes: a single formulation combining two anticancer treatments with enhanced therapeutic efficiency*. *J Clin Endocrinol Metab*, 2010. **95**(2): p. 943-52.
30. Hantel, C. and F. Beuschlein, *Xenograft models for adrenocortical carcinoma*. *Mol Cell Endocrinol*, 2016. **421**: p. 28-33.
31. Gazdar, A.F., et al., *Establishment and characterization of a human adrenocortical carcinoma cell line that expresses multiple pathways of steroid biosynthesis*. *Cancer Res*, 1990. **50**(17): p. 5488-96.
32. Logie, A., et al., *Establishment and characterization of a human adrenocortical carcinoma xenograft model*. *Endocrinology*, 2000. **141**(9): p. 3165-71.
33. Leibovitz, A., et al., *New human cancer cell culture lines. I. SW-13, small-cell carcinoma of the adrenal cortex*. *J Natl Cancer Inst*, 1973. **51**(2): p. 691-7.
34. Mariniello, B., et al., *Combination of sorafenib and everolimus impacts therapeutically on adrenocortical tumor models*. *Endocr Relat Cancer*, 2012. **19**(4): p. 527-39.
35. Demeure, M.J., et al., *Preclinical investigation of nanoparticle albumin-bound paclitaxel as a potential treatment for adrenocortical cancer*. *Ann Surg*, 2012. **255**(1): p. 140-6.
36. Siolas, D. and G.J. Hannon, *Patient-derived tumor xenografts: transforming clinical samples into mouse models*. *Cancer Res*, 2013. **73**(17): p. 5315-9.
37. Morton, C.L. and P.J. Houghton, *Establishment of human tumor xenografts in immunodeficient mice*. *Nat Protoc*, 2007. **2**(2): p. 247-50.
38. Pinto, E.M., et al., *Establishment and characterization of the first pediatric adrenocortical carcinoma xenograft model identifies topotecan as a potential chemotherapeutic agent*. *Clin Cancer Res*, 2013. **19**(7): p. 1740-7.
39. Beuschlein, F., et al., *IGF1-R inhibition and liposomal doxorubicin: Progress in preclinical evaluation for the treatment of adrenocortical carcinoma*. *Mol Cell Endocrinol*, 2016. **428**: p. 82-8.
40. Brase, J.C., et al., *Serum microRNAs as non-invasive biomarkers for cancer*. *Mol Cancer*, 2010. **9**: p. 306.
41. Wang, J., et al., *Tumor-associated circulating microRNAs as biomarkers of cancer*. *Molecules*, 2014. **19**(2): p. 1912-38.

42. Szabo, D.R., et al., *Analysis of circulating microRNAs in adrenocortical tumors*. Lab Invest, 2014. **94**(3): p. 331-9.
43. Cherradi, N., *microRNAs as Potential Biomarkers in Adrenocortical Cancer: Progress and Challenges*. Front Endocrinol (Lausanne), 2015. **6**: p. 195.
44. Duregon, E., et al., *MicroRNA expression patterns in adrenocortical carcinoma variants and clinical pathologic correlations*. Hum Pathol, 2014. **45**(8): p. 1555-62.
45. Patterson, E.E., et al., *MicroRNA profiling of adrenocortical tumors reveals miR-483 as a marker of malignancy*. Cancer, 2011. **117**(8): p. 1630-9.
46. Greither, T., et al., *Expression of microRNA 210 associates with poor survival and age of tumor onset of soft-tissue sarcoma patients*. Int J Cancer, 2012. **130**(5): p. 1230-5.
47. Greither, T., et al., *Elevated expression of microRNAs 155, 203, 210 and 222 in pancreatic tumors is associated with poorer survival*. Int J Cancer, 2010. **126**(1): p. 73-80.
48. Hong, L., et al., *High expression of miR-210 predicts poor survival in patients with breast cancer: a meta-analysis*. Gene, 2012. **507**(2): p. 135-8.
49. Li, Z.H., et al., *Prognostic significance of serum microRNA-210 levels in nonsmall-cell lung cancer*. J Int Med Res, 2013. **41**(5): p. 1437-44.
50. Huang, X., Q.T. Le, and A.J. Giaccia, *MiR-210--micromanager of the hypoxia pathway*. Trends Mol Med, 2010. **16**(5): p. 230-7.
51. Chan, Y.C., et al., *miR-210: the master hypoxamir*. Microcirculation, 2012. **19**(3): p. 215-23.
52. Berruti, A., et al., *Mitotane associated with etoposide, doxorubicin, and cisplatin in the treatment of advanced adrenocortical carcinoma. Italian Group for the Study of Adrenal Cancer*. Cancer, 1998. **83**(10): p. 2194-200.
53. Jung, S., et al., *Preclinical progress and first translational steps for a liposomal chemotherapy protocol against adrenocortical carcinoma*. Endocr Relat Cancer, 2016. **23**(10): p. 825-37.
54. Nagy, Z., et al., *Evaluation of 9-cis retinoic acid and mitotane as antitumoral agents in an adrenocortical xenograft model*. Am J Cancer Res, 2015. **5**(12): p. 3645-58.
55. Berruti, A., et al., *Adrenal cancer: ESMO Clinical Practice Guidelines for diagnosis, treatment and follow-up*. Ann Oncol, 2012. **23 Suppl 7**: p. vii131-8.

56. Ferrari L, C.M., Grisanti S, Berruti A, *Systemic Therapy in Locally Advanced or Metastatic Adrenal Cancers: A Critical Appraisal and Clinical Trial Update* European Urology Focus, 2016. **1**: p. 298-300.
57. Stathopoulos, G.P. and T. Boulikas, *Lipoplatin formulation review article*. J Drug Deliv, 2012. **2012**: p. 581363.
58. Allen, T.M. and P.R. Cullis, *Liposomal drug delivery systems: from concept to clinical applications*. Adv Drug Deliv Rev, 2013. **65**(1): p. 36-48.
59. Torchilin, V.P., *Recent advances with liposomes as pharmaceutical carriers*. Nat Rev Drug Discov, 2005. **4**(2): p. 145-60.
60. Ribeiro, R.C. and B. Figueiredo, *Childhood adrenocortical tumours*. Eur J Cancer, 2004. **40**(8): p. 1117-26.
61. Lalli, E. and B.C. Figueiredo, *Pediatric adrenocortical tumors: what they can tell us on adrenal development and comparison with adult adrenal tumors*. Front Endocrinol (Lausanne), 2015. **6**: p. 23.
62. Pinto, E.M., et al., *Genomic landscape of paediatric adrenocortical tumours*. Nat Commun, 2015. **6**: p. 6302.
63. Zancanella, P., et al., *Mitotane associated with cisplatin, etoposide, and doxorubicin in advanced childhood adrenocortical carcinoma: mitotane monitoring and tumor regression*. J Pediatr Hematol Oncol, 2006. **28**(8): p. 513-24.
64. Rodriguez-Galindo, C., et al., *Biology, clinical characteristics, and management of adrenocortical tumors in children*. Pediatr Blood Cancer, 2005. **45**(3): p. 265-73.
65. Tardi, P., et al., *Liposomal encapsulation of topotecan enhances anticancer efficacy in murine and human xenograft models*. Cancer Res, 2000. **60**(13): p. 3389-93.
66. Yu, Y., et al., *Mitochondrial targeting topotecan-loaded liposomes for treating drug-resistant breast cancer and inhibiting invasive metastases of melanoma*. Biomaterials, 2012. **33**(6): p. 1808-20.
67. Sengupta, S., et al., *Etoposide encapsulated in positively charged liposomes: pharmacokinetic studies in mice and formulation stability studies*. Pharmacol Res, 2000. **42**(5): p. 459-64.
68. Sengupta, S., et al., *Encapsulation in cationic liposomes enhances antitumour efficacy and reduces the toxicity of etoposide, a topo-isomerase II inhibitor*. Pharmacology, 2001. **62**(3): p. 163-71.
69. Miller, R.P., et al., *Mechanisms of Cisplatin nephrotoxicity*. Toxins (Basel), 2010. **2**(11): p. 2490-518.

70. Lipshultz, S.E., et al., *Late cardiac effects of doxorubicin therapy for acute lymphoblastic leukemia in childhood*. N Engl J Med, 1991. **324**(12): p. 808-15.
71. Steinherz, L.J., et al., *Cardiac toxicity 4 to 20 years after completing anthracycline therapy*. JAMA, 1991. **266**(12): p. 1672-7.
72. Devarajan, P., et al., *Low renal toxicity of lipoplatin compared to cisplatin in animals*. Anticancer Res, 2004. **24**(4): p. 2193-200.
73. Mettler, F.P., D.M. Young, and J.M. Ward, *Adriamycin-induced cardiotoxicity (cardiomyopathy and congestive heart failure) in rats*. Cancer Res, 1977. **37**(8 Pt 1): p. 2705-13.
74. O'Brien, M.E., et al., *Reduced cardiotoxicity and comparable efficacy in a phase III trial of pegylated liposomal doxorubicin HCl (CAELYX/Doxil) versus conventional doxorubicin for first-line treatment of metastatic breast cancer*. Ann Oncol, 2004. **15**(3): p. 440-9.
75. Balazsovits, J.A., et al., *Analysis of the effect of liposome encapsulation on the vesicant properties, acute and cardiac toxicities, and antitumor efficacy of doxorubicin*. Cancer Chemother Pharmacol, 1989. **23**(2): p. 81-6.
76. Stathopoulos, G.P., et al., *Pharmacokinetics and adverse reactions of a new liposomal cisplatin (Lipoplatin): phase I study*. Oncol Rep, 2005. **13**(4): p. 589-95.
77. Qiu, S., et al., *Interactions of miR-323/miR-326/miR-329 and miR-130a/miR-155/miR-210 as prognostic indicators for clinical outcome of glioblastoma patients*. J Transl Med, 2013. **11**: p. 10.
78. Muller, V., et al., *Changes in serum levels of miR-21, miR-210, and miR-373 in HER2-positive breast cancer patients undergoing neoadjuvant therapy: a translational research project within the Geparquinto trial*. Breast Cancer Res Treat, 2014. **147**(1): p. 61-8.
79. Chen, J., et al., *Predicting distant metastasis and chemoresistance using plasma miRNAs*. Med Oncol, 2014. **31**(1): p. 799.
80. Jung, E.J., et al., *Plasma microRNA 210 levels correlate with sensitivity to trastuzumab and tumor presence in breast cancer patients*. Cancer, 2012. **118**(10): p. 2603-14.
81. Andreoli, S.C., et al., *Use of microRNAs in directing therapy and evaluating treatment response in colorectal cancer*. Einstein (Sao Paulo), 2014. **12**(2): p. 256-8.
82. Libe, R., *Adrenocortical carcinoma (ACC): diagnosis, prognosis, and treatment*. Front Cell Dev Biol, 2015. **3**: p. 45.
83. Yardley, D.A., *Drug resistance and the role of combination chemotherapy in improving patient outcomes*. Int J Breast Cancer, 2013. **2013**: p. 137414.

84. Bukowski, R.M., et al., *Phase II trial of mitotane and cisplatin in patients with adrenal carcinoma: a Southwest Oncology Group study*. J Clin Oncol, 1993. **11**(1): p. 161-5.
85. Bonacci, R., et al., *Cytotoxic therapy with etoposide and cisplatin in advanced adrenocortical carcinoma*. Br J Cancer, 1998. **78**(4): p. 546-9.
86. Koukourakis, M.I., et al., *Concurrent liposomal cisplatin (Lipoplatin), 5-fluorouracil and radiotherapy for the treatment of locally advanced gastric cancer: a phase I/II study*. Int J Radiat Oncol Biol Phys, 2010. **78**(1): p. 150-5.

## 7. Appendix

### 7.1 Abbreviations

abbreviation	nomenclature
%	percentage
°C	celsius
µg/g	microgram per gram
µg/kg	microgram per kilogram
µl	microliter
µm	micrometer
ab	antibody
ACC	adrenocortical carcinoma
BON	BON cell line (human adrenocortical cancer cell line)
BSA	bovine serum albumin
bw	body weight
cel-miR 39	caenorhabditis elegans microRNA 39
cm	centimeter
cm <sup>2</sup>	square centimeter
cm <sup>3</sup>	cubic centimeter
dest.	distilled
DMEM/F12	dulbecco's modified eagle's medium
DU-145	DU-145 cell line (prostate cancer cell line)
EDP-M	etoposide, doxorubicin, cisplatin and mitotane
EDTA	ethylenediaminetetraacetic acid
ENSAT	european network for the study of adrenal tumors
EPR-effect	enhanced permeability and retention effect
EtOH	ethanol
fig.	figure
FIRM-ACT	First International Randomized trial in locally advanced and Metastatic Adrenocortical Carcinoma Treatment

abbreviation	nomenclature
g	gram
g/kg	gram per kilogram
G/L	giga per liter
h	hour
H <sub>2</sub> O <sub>2</sub>	hydrogen peroxide
HCl	hydrochloric acid
HIF-1 $\alpha$	hypoxia-inducible factor 1 $\alpha$
HPF	high-power field, 400x magnification, 0.391 mm <sup>2</sup>
i.m.	intramuscular
i.p.	intraperitoneal
i.v.	intravenous
IGF2 gene	insulin growth factor 2 gene
ITS	insulin-transferrin selenium
Kelly	Kelly cell line (human neuroblastoma cell line)
kg	kilogram
Ki67	human protein encoded by the MKI67 gene, used as proliferation marker
l	liter
L(I)EDP-M	liposomal etoposide, liposomal doxorubicin, liposomal cisplatin and mitotane
l/min	flow-rate, liter per minute
LEDP-M	etoposide, liposomal doxorubicin, liposomal cisplatin and mitotane
M	molar
mg	milligram
MgSO <sub>4</sub> *7H <sub>2</sub> O	magnesiumsulfateheptahydrate
min.	minute
miR	microRNA
miR-210	microRNA 210
miR-483-5p	microRNA 483-5p
ml	milliliter
mM	millimolar
MUC-1	MUC-1 xenograft model (adult adrenocortical carcinoma)
n	number

abbreviation	nomenclature
NaCl	sodium chloride
NaHCO <sub>3</sub>	Sodium bicarbonate
NaOH	sodium hydroxide
NCI-H295R	NCI-H295R cell line (human adrenocortical cancer cell line)
nm	nanometer
NMRI nu/nu	NMRI nude mouse strain
<i>o,p'</i> DDD	mitotane (1-( <i>o</i> - chlorophenyl)-1-( <i>p</i> -chlorophenyl)-2,2-dichloroethane)
P/S	penicillin/streptomycin
PBS	phosphate buffered saline
PEG	polyethylene glycol
PPE	palmar-plantar erythrodysesthesia
qRT-PCR	quantitative Real-Time PCR
r/min	rotations per minute
RNA	ribonucleic acid
RT-qPCR	quantitative real-time PCR
s.c.	subcutaneous
SD	standard deviation
SEM	standard error of the mean
SJ-ACC3	SJ-ACC3 xenograft model (pediatric adrenocortical carcinoma)
SW-13	SW-13 cell line (human adrenocortical cancer cell line, derived from small-cell carcinoma of the adrenal gland)
Sz-M	streptozotocin, mitotane
VEGF	vascular endothelial growth factor
vs.	versus

## 7.2 Acknowledgements

Ich möchte mich an erster Stelle bei meinem Doktorvater Prof. Dr. Felix Beuschlein und bei meiner („inoffiziellen“) Doktormutter Dr. Constanze Hantel bedanken. Vielen Dank, dass ihr beide immer ein offenes Ohr für mich hattet und mich zu jeder Zeit unterstützt habt. Ich danke euch für eure ermutigenden Worte, für die unkomplizierte Betreuung und vor allem für die immerwährende Unterstützung in meinem Studium und meiner weiteren Laufbahn.

Ich möchte mich zudem bei den Kooperationspartnern bedanken, ohne eure Unterstützung wäre dieses Projekt in dieser Form nicht zustande gekommen. Prof. Dr. Martin Fassnacht möchte ich in aller Form dafür danken, es mit Prof. Dr. Felix Beuschlein ermöglicht zu haben, erste Patientendaten in dieses Projekt einschließen zu können. Mein Dank geht außerdem nach Ungarn an Prof. Dr. Peter Igaz und Dr. Zoltan Nagy, die mich für meine microRNA Analysen mit offenen Armen in ihr Labor in Budapest aufgenommen haben. Ein großes Dankeschön geht an Dr. Max Weiss, danke für Ihre fachliche Kompetenz und die unkomplizierte und im wahrsten Sinne „herzliche“ Zusammenarbeit. Danke an Prof. Martin Reincke, dass Sie dieses Projekt immer unterstützt haben. Ebenfalls möchte ich mich bei HRA Pharma, Tani Boulikas und dem Team von Gerard Zambetti für die Bereitstellung von Mitotane, Lipoplatin und dem SJ-ACC3 Tumormodell bedanken.

Neben meinem Doktor“vater“, meiner Doktor“mutter“ möchte ich aber auch vor allem bei meiner Doktor“familie“ bedanken: Danke an Susanne und Igor, ihr habt mich immer unterstützt und ich habe mich immer auf euch verlassen können. Auch den Labor“mamas“ Brigitte und Petra möchte ich meinen Dank aussprechen, dass ihr egal in welchen Lebenslagen immer für mich da seid, ich werde diese schöne Zeit mit euch nicht vergessen. Danke außerdem an Ayse, Christina, Christian, Guido, Jessie, Kerstin, Ludwig, Luis, Marion, Tracy, Yara, Yiqing und allen anderen, die ich hier nicht namentlich erwähne, ihr wart nicht nur meine Kollegen sondern seid meine Freunde geworden, danke für eure Unterstützung und eure Fröhlichkeit, ihr seid ein tolles Team! Neben unserer Labormannschaft möchte ich mich außerdem bei den Mitarbeitern der ZVH bedanken, danke an das ganze Team und vor allem Ira und Frau Dr. Annalena Riedasch, dass ihr mich immer unterstützt habt und immer ein offenes Ohr für mich hattet.

Zuletzt möchte ich mich bei meiner Familie, meinen Großeltern und bei meinen Freunden aus tiefsten Herzen bedanken, ohne euch wäre ich heute nicht da, wo ich jetzt bin. Ihr unterstützt mich bei allem, was ich mir in den Kopf setze. Danke für die Kraft, die ihr mir gebt!

